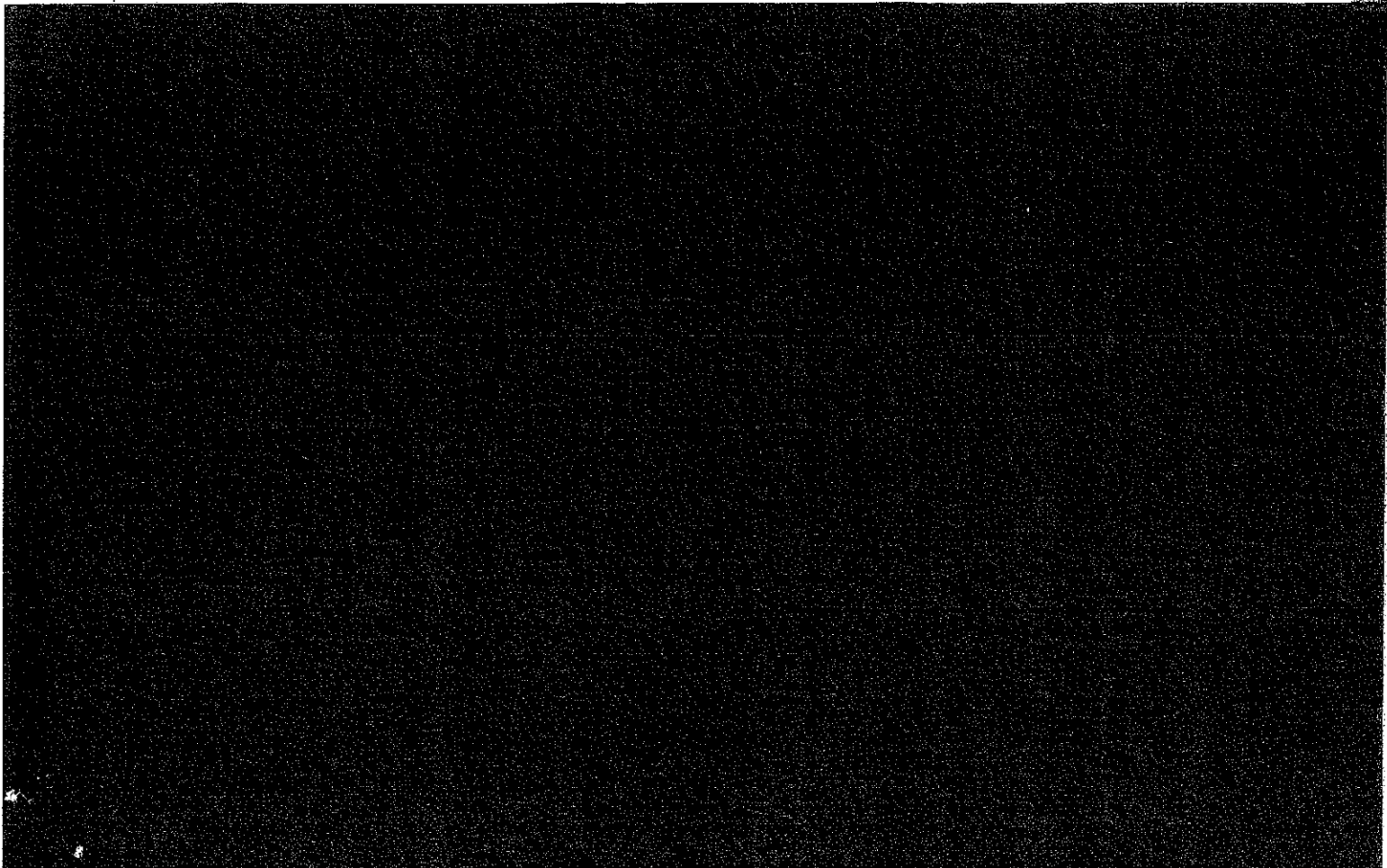


MOMENT-BASED HERMITE MODELS OF RANDOM VIBRATION

Steven R. Winterstein

March, 1987



ABSTRACT

Moment-based Hermite models of nonlinear random vibration are formulated. These models use N response moments (skewness, kurtosis, etc.) to construct N non-Gaussian contributions, made orthogonal through a Hermite series. Models of both hardening and softening nonlinear behavior are developed. In both cases the Hermite models are shown to be more flexible than the commonly used Charlier and Edgeworth series, with the ability to reflect wider ranges of nonlinear behavior. Analytical results are derived for spectral densities, crossing rates, probability distributions of the response and its extremes, and fatigue damage rates. These are found to compare well with exact results for various nonlinear models, including nonlinear oscillator responses and quasi-static responses to non-Gaussian (Morison) wave loads.

RESUME

Momentbaserede Hermite modeller for ikke lineare stokastiske svingninger er formuleret. Modellerne anvender N responsmomenter (skævhed, kurtosis, etc.) til at konstruere N indbyrdes ortogonale ikke Gaussiske bidrag, der indgår som led i en Hermite række. Modeller for både hård og blød ikke lineær opførsel er udviklet. For begge tilfælde vises, at Hermite modellerne er mere fleksible end de gangse Charlier og Edgeworth rækker, og at de kan reflektere et bredere spektrum af ikke lineær opførsel. Der udledes analytiske resultater for spektraltætheder, krydsningsintensiteter, sandsynlighedsfordelinger af responset og dets ekstremer, og skadeakkumuleringshastighed vedrørende udmattelse. Resultaterne stemmer overens med exakte resultater for forskellige ikke lineære modeller, inklusive respons fra ikke lineære oscillatorer, og quasi-statisk respons på ikke Gaussiske (Morison) bølgelaster.

Moment-based Hermite Models of Random Vibration

Copyright © by Steven R. Winterstein 1987

Tryk:

Afdelingen for Bærende Konstruktioner

Danmarks Tekniske Højskole

Lyngby

ISBN 87-87336-78-2

MOMENT-BASED HERMITE MODELS OF RANDOM VIBRATION

by Steven R. Winterstein¹

TABLE OF CONTENTS

INTRODUCTION	1
Approximating Nonnormal Responses	2
GRAM-CHARLIER AND EDGEWORTH SERIES	3
MOMENT-BASED HERMITE MODELS FOR NONLINEAR RESPONSES	8
Softening Response Statistics from Implicit Hermite Series	8
Model Calibration from Central Moments	10
Explicit Hermite Models of Hardening Responses	13
Application to Nonlinear Oscillators	14
SPECTRA, LOCAL AND GLOBAL EXTREMES, AND FATIGUE	18
Response Covariance and Spectral Density	18
Global Extrema and First-Passage Failures	18
Local Response Extrema	19
Response Envelopes and Ranges	20
Fatigue Damage Rates	21
HERMITE MODELS OF MORISON WAVE FORCES	23
SUMMARY AND CONCLUSIONS	27
Acknowledgements	27
References	28
Appendix A: ORTHOGONAL EXPANSIONS FOR RANDOM PROCESSES	A-1
Appendix B: INCLUDING DEPENDENCE AND NONSTATIONARITY IN MOMENT-BASED ESTIMATES OF UPCROSSING RATES	B-1

INTRODUCTION

To assess structural reliability against extreme loads and fatigue, dynamic responses are commonly modelled as Gaussian random processes. This model is generally inappropriate, however, when structural behavior is nonlinear, the excitation is non-Gaussian (e.g., wind and wave loads), or both. In such cases, conventional linear/Gaussian models may significantly misrepresent the frequency of large response levels, which contribute most to both first-passage (Grigg, 1984a, 1984b) and fatigue failures (Lutes et al., 1984). Simple analytical results are developed here to predict these nonlinear effects, using Hermite series models based on response moments.

Various nonlinear models have been formulated through series approximations, often in terms of Hermite polynomials. The series of Charlier (1905) and Edgeworth (1907) have often been used in nonlinear problems to estimate full probability distributions from a limited number of response moments (e.g., Grandall, 1980; Muratsu et al., 1981; Ochi, 1986; Soize, 1978). Nonetheless, these series can behave erratically, yielding multimodal and even negative probability densities and crossing rates for significant nonlinearities. These series can be truncated (Ochi, 1986) or otherwise modified (Muratsu et al., 1981) to avoid this undesirable behavior; however, the resulting tail behavior is somewhat arbitrary and fails to preserve the given moments. Alternatively, a nonlinearity of known functional form (e.g., nonlinear force-deflection curve) can be expanded into a Hermite series to reflect nonlinear contributions to the response covariance and spectral density (Madsen, 1986). This method requires an analytical description of the nonlinearity, and is not generally used to reflect non-Gaussian response characteristics.

The moment-based Hermite models defined here use N response moments (skewness, kurtosis, etc.) to construct N non-Gaussian contributions, made orthogonal through a Hermite series. Using observed moments from a response time history, these Hermite models permit simple analytical corrections for nonlinear effects, without the need to fully specify or analyze a precise nonlinear model. These models are hence well-suited for nonlinear system identification, analogous to a Wiener power series based on higher-order cross-spectra of load

¹Acting Asst. Prof., Dept. of Civ. Engrg., Stanford Univ., Stanford, Calif.

and response (Schetzen, 1980). The necessary moments can also be estimated analytically, for example, through closure schemes for nonlinear responses to white noise (Crandall, 1980; Wu and Lin, 1984), and through general input-output relations for higher moments of linear responses to non-Gaussian input (Lin, 1976; Lutes and Hu, 1986).

These Hermite models are shown to be more flexible than the Charlier and Edgeworth series, with the ability to reflect a wider range of nonlinear behavior. They are also particularly tractable, reducing nonlinear analysis in many cases to simple transformation of known results from linear (Gaussian) theory. Analytical results are derived for spectral densities, crossing rates, probability distributions (of the response, its peaks, ranges, and extremes), and fatigue damage rates. These are found to compare well with the exact results for various nonlinear models, including functionally-transformed Gaussian processes, nonlinear oscillator responses, and quasi-static responses to non-Gaussian (Morison) wave loads.

Approximating Nonnormal Responses.—It is useful in various applications to estimate $\nu_X(x)$, the mean rate at which the stationary response $X(t)$ crosses level x from below. Defining $\nu_0 = \max[\nu_X(x); -\infty < x < +\infty]$ as the rate of response "cycles," the normalized rate $\nu_X(x)/\nu_0$ approximates both the failure rate per cycle (for extremes) and the probability that a response peak exceeds level x in narrow-band vibration (for fatigue). Unfortunately, in practice $\nu_X(x)$ may be unavailable because the precise form of nonlinearity is either unknown or analytically intractable. In these cases minimal information to construct non-Gaussian models is provided by response moments, e.g., the skewness and kurtosis coefficients, α_3 and α_4 ($\alpha_n = E\{[X(t) - \bar{m}_X]^n / \sigma_X^n$).

Clearly, the dynamic behavior described by $\nu_X(x)$ is not uniquely determined by the entire probability density function (PDF) of $X(t)$. $\nu_X(x)$, let alone by a limited number of central moments. Two assumptions are effectively required: one regarding the static nature of the response (to estimate $f_X(x)$ from moments) and a second concerning dynamic behavior (to infer $\nu_X(x)$ from $f_X(x)$). Considering the dynamic problem first, two simple estimates of $\nu_X(x)/\nu_0$ from $f_X(x)$ are

$$\frac{\nu_X(x)}{\nu_0} = \begin{cases} \frac{f_X(x)}{f_X(\bar{m}_X)} & (1a) \\ \exp\{-\frac{1}{2}[g^{-1}(x)]^2\} & (1b) \end{cases}$$

in which \bar{m}_X denotes the response mode, for which $f_X(x)$ is maximized. Eq. 1a follows if the quantities $\dot{X}(t)$ and $\dot{X}(t)$, which are uncorrelated, are assumed independent as well. Alternatively, Eq. 1b assumes that $X(t) = g(U(t))$, a functional transformation of the standard normal process $U(t)$; $g'(u) = F_X^{-1}[\phi(u)]$ and $g^{-1}(x) = \phi^{-1}[F_X(x)]$ in terms of the cumulative distribution functions, F_X and ϕ , of $X(t)$ and $U(t)$. While these two assumptions are not satisfied simultaneously for nonlinear (nonnormal) responses, either of the two leads to flexible yet tractable models.

When only central moments of $X(t)$ are available, Eq. 1a is a natural choice in view of the widely-used Charlier and Edgeworth series for $f_X(x)$ based on these moments (Johnson and Kotz, 1970). It is shown in the next section, however, that when these series are based on a moderate number of moments, they may not accurately reflect significant nonlinearities. In the following section, an alternative model is derived by approximating g in Eq. 1b, rather than f_X in Eq. 1a, from central moments. Hermite series estimates of g and of g^{-1} are shown to provide useful models of softening ($\alpha_4 > 3$) and hardening ($\alpha_4 < 3$) responses, respectively. These Hermite series models are as simple to apply as the Charlier results; indeed the same coefficients may arise, albeit in a different role. These Hermite models are generally more stable, however, avoiding the possibility of negative PDFs and crossing rates. In the final section, these Hermite models are used to develop simple moment-based results to predict nonlinear effects on the response covariance, extremes, ranges, and fatigue damage.

GRAM-CHARLIER AND EDGEWORTH SERIES

It is convenient to consider the standardized response $X_0(t) = [X(t) - \bar{m}_X] / \sigma_X$, whose PDF can be expanded to match N moments as follows (Appendix A):

$$f_{X_0}(x_0) = \varphi(x_0) \left\{ 1 + \sum_{n=1}^N h_n H_n(x_0) \right\} \quad (2)$$

in terms of the standard normal PDF, $\varphi(x_0) = (2\pi)^{-1/2} \exp(-x_0^2/2)$, and the Hermite polynomials $H_n(x_0)$. For example, $H_0(x_0) = 1$, $H_1(x_0) = x_0$, $H_2(x_0) = x_0^2 - 1$, $H_3(x_0) = x_0^3 - 3x_0$, and $H_4(x_0) = x_0^4 - 6x_0^2 + 3$. It is readily shown (Appendix A) that the coefficients h_n are directly related to the response moments, and are defined here as "Hermite moments":

$$h_n = \frac{1}{n!} E[H_n(X_0)] \quad (3)$$

While these results do not require a standardized response of zero mean and unit variance, convergence of Eq. 2 generally requires more terms for non-

standardized responses.

Expanding $H_n(X_0)$ as a power series in X_0 and vice versa, h_n can be related to the central moments, $\alpha_n = E[X_0^n(t)]$:

$$h_n = \frac{\alpha_n}{n!} - \frac{\alpha_{n-2}}{1!2!(n-2)!} + \frac{\alpha_{n-4}}{2!2^2!(n-4)!} - \dots \quad (4a)$$

$$\alpha_n = n! \left\{ h_n + \frac{h_{n-2}}{1!2} + \frac{h_{n-4}}{2!2^2} + \dots \right\} \quad (4b)$$

For example, $h_1 = h_3 = 0$ for all standardized responses while $h_5 = \alpha_5/6$ and $h_4 = (\alpha_4 - 3)/24$, proportional to the skewness and the coefficient of excess, respectively. While reflecting the same information as the central moments α_n , these Hermite moments are more direct measures of nonlinearity. The quantities $n!h_n\sigma_0^2$ are identical to response cumulants for $n \leq 5$, and to the quasi-moments of Stratonovich (1963) for $n \leq 7$. For linear (Gaussian) responses $h_n = 0$ for all $n > 0$.

By truncating Eq. 2 at $n=N$, one effectively assumes h_n to be negligible for $n > N$. Only the first $N=4$ moments are typically used in data applications, because higher moments may show large sampling variability. Combining Eqs. 1a and 2 and truncating at $N=4$,

$$\frac{\nu_X(x)}{\nu_X(m_X)} = \exp\left(-\frac{x^2}{2}\right) \left\{ \frac{1 + h_3(x_0^2 - 3x_0) + h_4(x_0^4 - 6x_0^2 + 3)}{1 + 3h_4} \right\} \quad (5)$$

in which $x_0 = (x - m_X)/\sigma_X$. This is consistent with the conventional four-moment Charlier series for $f_X(x)$. The corresponding Edgeworth series, which assumes that response cumulants decay in a specific fashion, retains an additional term for asymmetric responses (Johnson and Kotz, 1970).

Various extensions of this result are possible. Additional terms may be retained in Eq. 2 to reflect marginal response moments of still higher orders (again, Eq. 2 may depart from classical results that ignore higher-order cumulants, rather than Hermite moments). Joint Hermite moments of X and \dot{X} , $h_{nm} = E[H_n(X)H_m(\dot{X})]/n!m!$, may also be used to relax the assumption that these variables are independent. Applying Rice's formula to an expansion of $f_{X\dot{X}}(x, \dot{x})$ analogous to Eq. 2, $\nu_X(x)$ is found to be

$$\nu_X(x) = \frac{1}{2\pi} \exp\left(-\frac{x^2}{2}\right) \sum_{n=0}^{\infty} c_n H_n(x) \quad (6a)$$

in which

$$c_n = h_{n0} + \sum_{m=0}^{\infty} \frac{2m!}{m!} \left(-\frac{1}{2}\right)^m h_{n,2m+2} \quad (6b)$$

This result is derived in Appendix B, along with more general results that include nonstationary responses and time-varying thresholds. The impact of these additional corrections may not be sufficient, however, to justify the additional effort needed to accurately estimate these higher moments.

Significantly, Eq. 2 may be viewed as a polynomial approximation to the ratio of PDFs, $f_{X_0}(x_0)/\varphi(x_0)$. If few higher moments are retained, $f_{X_0}(x_0)/\varphi(x_0)$ is approximated by a low-order polynomial and the resulting tail behavior of $f_X(x)$ (and of $\nu_X(x)$ in Eq. 1a) is not markedly different than that of the Gaussian model. Because its tail behavior is so inflexible, Eq. 2 may produce an ill-behaved estimate of $f_X(x)$ — multimodal and even negative — in order to reproduce the moments of a significantly nonlinear response.

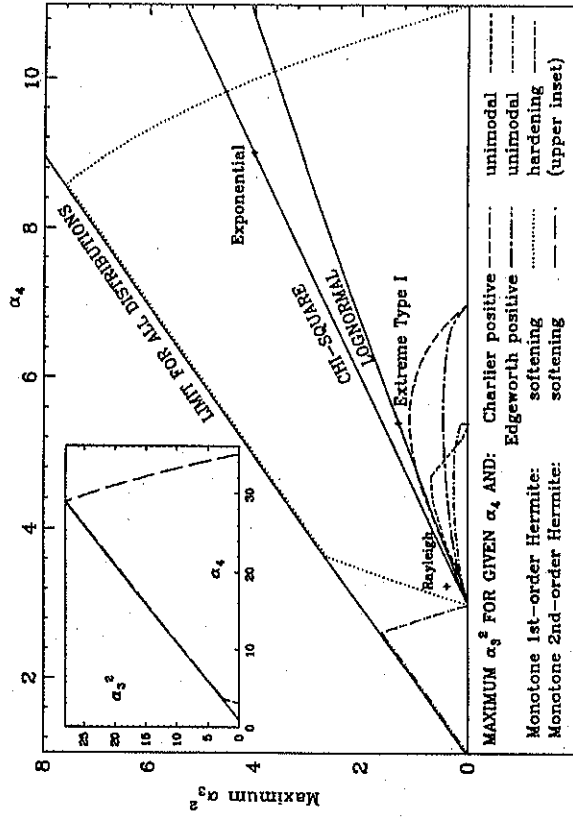


Figure 1: Values of skewness and kurtosis accurately represented by various models.

This situation is illustrated in Figs. 1 and 2. Fig. 1 shows the limited range of α_3 and α_4 for which the four-moment Charlier series (Eq. 2 with $N=4$ and Eq. 5) and its Edgeworth variant are (i) positive and (ii) unimodal. In both cases, the region of unimodal behavior is the smaller of the two. (The respective regions are bounded by the curves shown, which represent maximum possible α_3^2 values, and the $\alpha_3=0$ axis.) The (α_3, α_4) values of various common distributions are also shown for reference: the lognormal and chi-square distributions correspond to lines on this diagram, while other distributions (e.g., Rayleigh, exponential, type I extreme value) represent only single points. Although the Charlier series shows greater stability than the Edgeworth model, neither produces a positive definite $f_X(x)$ for any hardening response ($\alpha_4 < 3, h_4 < 0$). The extent of softening (positive values of h_4) and asymmetry (nonzero values of h_3) that can be modelled acceptably is also limited; of the common distributions shown, only a lognormal with relatively small coefficient of variation can be realistically modelled.

Even if these series provide unimodal estimates of $f_X(x)$ and $\nu_X(x)$, they may fail to reflect significantly nonlinear (non-Gaussian) behavior. This is illustrated by Fig. 2, which shows Charlier results (Eq. 5) for symmetric responses whose fourth moments increase through $\alpha_4=5$ ($h_4=1/12$). Also shown are exact results for various nonlinear transformations of a Gaussian process $U(t)$; the nonlinear parameter c in Fig. 2 has been adjusted to produce the desired fourth moment. As α_4 increases, the Charlier results retain the characteristic Gaussian-like shape, parabolic on the semi-log scale shown. This produces systematic and unconservative errors in estimating tail behavior. Even for moderate response levels, Charlier estimates of $\nu_X(x)$ and $f_X(x)$ become increasingly erratic (yet unimodal, falling within the acceptable regions of Fig. 1 for the cases shown) as α_4 grows.

Note also that the various exact results in Fig. 2 show relatively little scatter. This suggests that, at least for transformed Gaussian models, four moments are sufficient to capture a great deal of the response's non-Gaussian characteristics. As the other curves in Fig. 2 anticipate, these characteristics are often better predicted by the Hermite models described below.

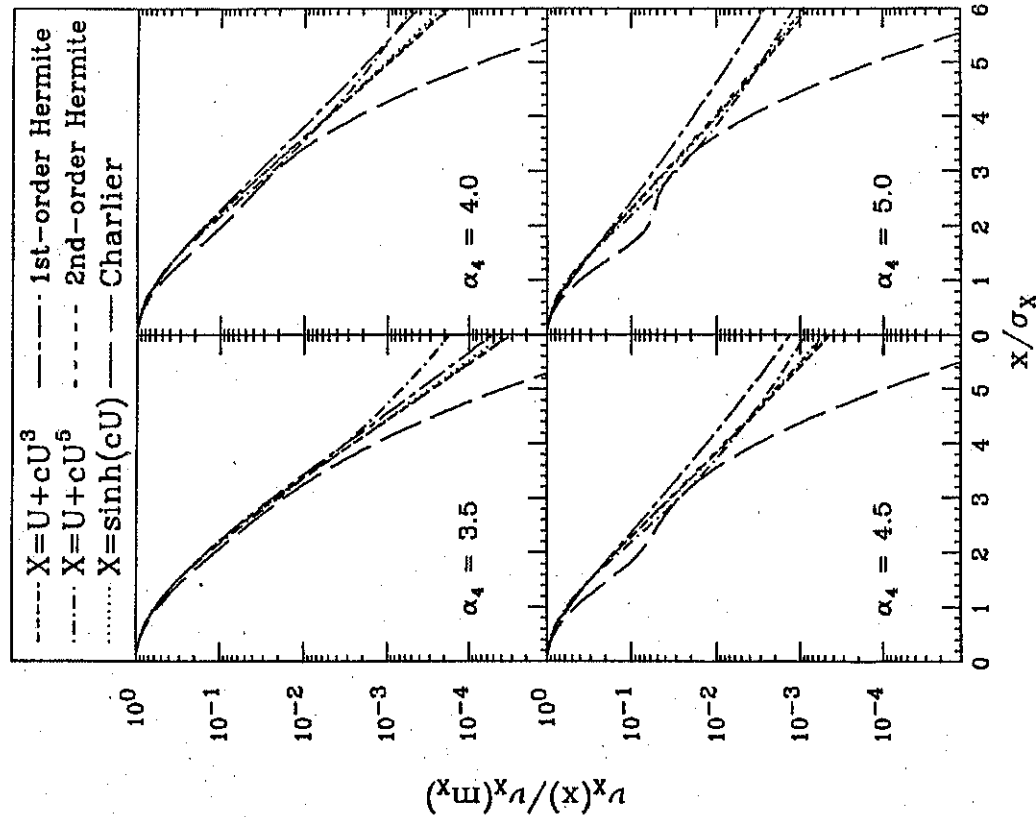


Fig. 2. Crossing rates of softening transformations of normal processes.

MOMENT-BASED HERMITE MODELS FOR NONLINEAR RESPONSES

The marginal distribution of virtually any structural response can be matched by applying an appropriate monotone function, g , to a normal process. For responses whose distributions have wider tails than the Gaussian ("softening" responses), $g(u)$ will be convex ($g'' > 0$) for large u . In these cases (e.g., $\alpha_4 > 3$), monotone polynomial approximations to g are constructed below from response moments. Because these approximations to g give only implicit estimates of the transformation to normality, $U(t) = g^{-1}(X_0(t))$, they are said here to give "implicit" models. (The need to calculate g^{-1} rather than g arises in various analytical results; e.g., Eq. 1b for $\nu_X(x)$.)

In contrast, $g(u)$ will be concave ($g'' < 0$) for large u if $X(t)$ is a "hardening" response, with narrower PDF than the Gaussian. It is difficult to construct polynomials that are both monotonically increasing and asymptotically concave; in these cases an explicit polynomial approximation to $g^{-1}(x) = \Phi^{-1}[F_X(x)]$ is more appropriate. These explicit hardening models are also developed from central moments in this section. (In addition to hardening systems under Gaussian loads, these hardening models apply for any input-system characteristics that produce responses with hardening characteristics; e.g., $\alpha_4 \leq 3$. The softening models are equally general.)

Softening Response Statistics from Implicit Hermite Series.— Given N response moments of a softening response, the transformation g to a standardized response is taken as an N -term Hermite series:

$$\begin{aligned} \frac{X(t) - m_X}{\sigma_X} &= X_0(t) + \sum_{n=3}^N \tilde{h}_n H e_{n-1}(U(t)) \\ &= \kappa [U(t) + \tilde{h}_3(U^2(t) - 1) + \tilde{h}_4(U^3(t) - 3U(t)) + \dots] \end{aligned} \quad (7)$$

The coefficients \tilde{h}_n control the shape of the standardized distribution, while κ is a scaling factor ensuring that $X_0(t)$ has unit variance. (The notation \tilde{h}_n reflects that these coefficients are roughly equal to the Hermite moments h_n — cf. Eqs. 13-14.) Because $H e_n(u) = \gamma_n H e_{n-1}(u)$, Eq. 7 will be monotone if

$$\frac{dX}{dX_0} = [\kappa (1 + \sum_{n=3}^N (n-1) \tilde{h}_n H e_{n-2}(u))]^{-1} > 0 \quad (8a)$$

for all u . Values of \tilde{h}_n for which Eq. 8a holds follow from its discriminant; e.g., if $N=4$ moments are fit, Eq. 8a leads to the condition

$$\tilde{h}_3^2 < 3\tilde{h}_4(1 - 3\tilde{h}_4) \quad (8b)$$

If the Hermite series in Eq. 7 is monotone, its crossing statistics and first-order probability distributions follow directly:

$$\nu_X(x) = \nu_{X_0}(x_0) = \nu_0 \exp\left(-\frac{u^2}{2}\right) \quad (9)$$

$$F_X(x) = F_{X_0}(x_0) = \Phi(u) \quad (10)$$

$$f_X(x) \sigma_X = f_{X_0}(x_0) = \varphi(u) \frac{du}{dx_0} \quad (11)$$

in which x_0 and dx_0/du are given in terms of u in Eqs. 7 and 8a. Because these results depend explicitly on u , their application for a specified response level x_0 requires that Eq. 7 be inverted to find $u(x_0) = g^{-1}(x_0)$. (Eq. 11 also requires inversion of Eq. 8a.) While this inversion must generally be performed numerically, explicit results for $g^{-1}(x_0)$ (and hence for Eqs. 9-11) can be found if no more than $N=5$ moments are to be matched. If $N=4$ moments are used, for example, Eq. 7 gives a cubic equation for $U(t)$ whose explicit solution is

$$U = \xi(X_0) \left[(1 + \psi(X_0))^{1/3} + (1 - \psi(X_0))^{1/3} \right] - a \quad (7')$$

in which

$$\xi(X_0) = \left[1.5b(a + X_0 - a^3) \right]^{1/3}; \quad \psi(X_0) = \left[1 + \left(\frac{b - 1 - a^2}{\xi^2(X_0)} \right)^{3/2} \right]^{1/2}$$

in terms of the constants $a = \tilde{h}_3/3\tilde{h}_4$ and $b = 1/3\tilde{h}_4$.

For design against vibration-induced failure, it is also useful to note that general explicit results can be derived for arbitrary fractiles of the nonlinear response. Defining x_p and m_p as the upper p -fractiles of the first-order distribution and crossing rate functions, $1 - F_X(x_p) = \nu_X(m_p)/\nu_0 = p$ in which

$$x_p = m_p + \kappa \sigma_X \left[-\Phi^{-1}(p) + \sum_{n=3}^N \tilde{h}_n H e_{n-1}(-\Phi^{-1}(p)) \right] \quad (12a)$$

$$m_p = m_p + \kappa \sigma_X \left[\sqrt{-2 \ln(p)} + \sum_{n=3}^N \tilde{h}_n H e_{n-1}(\sqrt{-2 \ln(p)}) \right] \quad (12b)$$

Eq. 12a is somewhat analogous to a Cornish-Fisher expansion for random variable fractiles (Johnson and Kotz, 1970), although these typically include additional non-Hermite polynomials based on the Edgeworth assumption regarding cumulants.

As the bandwidth of $X(t)$ decreases, $\nu_X(x)/\nu_0$ approaches the probability that an arbitrary response peak exceeds x , and m_p in Eq. 12b gives the upper p -fractile of response maxima. In the linear case, $\tilde{h}_n = 0$ for all $n \geq 3$ and $\kappa = 1$ so that Eqs. 12a-b yield fractiles of Gaussian and Rayleigh distributions, consistent with

linear theory for lightly damped responses. The effect of bandwidth on nonlinear response peaks is shown in Eq. 31. It suggests that Eq. 12b is conservative for high fractiles (small p), and that it can be improved by replacing p in its right-hand side by $p\nu_m/\nu_0$ (ν_m =rate of maxima).

Model Calibration from Central Moments.—To calibrate these results, the coefficients h_n and κ may be related to the Hermite moments h_n by applying a Hermite polynomial to Eq. 7 and taking expectations. This leads to a simultaneous set of nonlinear equations for the unknown coefficients h_n , which is generally difficult to solve. Results simplify considerably if second-order non-Gaussian contributions (i.e., terms of order $h_m h_n$) can be neglected (*Winterstein, 1985*):

$$\kappa = 1; \quad h_n = h_n \quad (n=3, 4, \dots) \quad (13)$$

Eqs. 7 and 13 are defined here as "first-order" softening (or implicit) Hermite models, as they match the actual moments to first order in the non-Gaussian contributions. As with the Charlier series in Eq. 2, the Hermite moments h_n again appear as coefficients that scale the non-Gaussian correction terms. Unlike Eq. 2, however, the polynomial moment-based corrections are used here to estimate g rather than $f_{X_0}(x_0)/\phi(x_0)$. This produces a significantly more flexible nonlinear model, as shown in Figs. 1 and 2 for $N=4$ moments. Fig. 1 shows that the first-order Hermite model behaves acceptably (monotonically, satisfying Eq. 6) for a considerably wider range of nonlinear responses than the Charlier and Edgeworth series. The corresponding estimate of $\nu_X(x)$ from the Hermite model (Eqs. 9 and 13) is found in Fig. 2 to better predict the exact results for various transformed normal responses. Unlike the Charlier and Edgeworth results, the Hermite model reflects the correct transition from logarithmic to roughly log-linear tail behavior as the nonlinearity increases.

Note also from Fig. 2 that as α_4 grows, the first-order Hermite model provides an increasingly conservative estimate of $\nu_X(x)$. Because the dynamic assumption in Eq. 1b is satisfied by the exact results, the source of error lies in the static modelling; i.e., in fitting a static distribution $f_{X_0}(x_0)$ that only reproduces moments to first order. If $O(h_m h_n)$ terms are also included in matching the moments of Eq. 7, the coefficients h_n are found to satisfy the simultaneous quadratic equations (Appendix A):

$$h_{p+2} = h_{p+2} + \frac{1}{2} \sum_{j=0}^p \frac{1}{j!(p-j)!} \sum_{k=3}^{N-|p-2j|} \frac{(k-1)!(k-1+|p-2j|)!}{[k-1-(p-|p-2j|)/2]!} h_k h_{k+|p-2j|} \quad (14a)$$

for $1 \leq p \leq N-2$. In terms of the coefficients h_n , the correct (unit) variance is obtained by choosing the scaling factor

$$\kappa = \left[1 + \sum_{n=3}^N (n-1) h_n^2 \right]^{-1/2} \quad (14b)$$

Eqs. 14a-b reduce to Eq. 13 if second-order terms are neglected.

An approximate solution for h_n in Eq. 14a follows by summing only over $k \geq p+2$, giving h_{p+2} in terms of $h_{p+2}, h_{p+3}, \dots, h_N$. Back substitution then yields the h_n values in decreasing order. With $N=4$, this procedure leads to the coefficients

$$h_4 = \frac{\sqrt{1+5(\alpha_4-3)}-1}{18} = \frac{\sqrt{1+36h_4}-1}{18}$$

$$h_3 = \frac{\alpha_3}{6(1+6h_4)} = \frac{h_3}{1+6h_4}$$

$$\kappa = [1 + 2h_3^2 + 6h_4^2]^{-1/2} \quad (15)$$

If $\alpha_3=0$, Eq. 15 ensures that the first three moments are matched exactly, and errors in the fourth Hermite moment (i.e., the coefficient of excess) are only of order h_4^3 . Larger errors in skewness and kurtosis are theoretically possible if $\alpha_3 \neq 0$; however, Eq. 15 is shown below to yield very good results for significantly skewed responses (Fig. 3). Combinations of Eq. 7 and Eq. 15 (or analogous results for larger values of N) are defined here as "second-order" softening Hermite models.

By matching response moments more accurately, these second-order Hermite models may better reflect significant nonlinearities than their first-order counterparts. Fig. 1 shows that the second-order models remain monotonic, satisfying Eqs. 8 and 15, over a much larger range of central moments. For central moments in this range, Eqs. 9-12 give response statistics in terms of the coefficients h_n from Eq. 15. These statistics avoid the systematic conservatism of the first-order Hermite estimates of $\nu_X(x)$ in Fig. 2. Even lognormal processes, whose non-Gaussian aspects increase rapidly with the coefficient of variation V , are relatively well-modelled by the second-order Hermite model (Fig. 3). In contrast, neither the Charlier nor Edgeworth series is able to model the lognormal's long upper tail. (All lognormal approximations are based on the moments $\sigma_3 = V(3+V^2)$ and $\sigma_4 = 3+V^2(16+15V^2+6V^4+V^6)$; the Charlier and Edgeworth results differ in this case due to response asymmetry.)

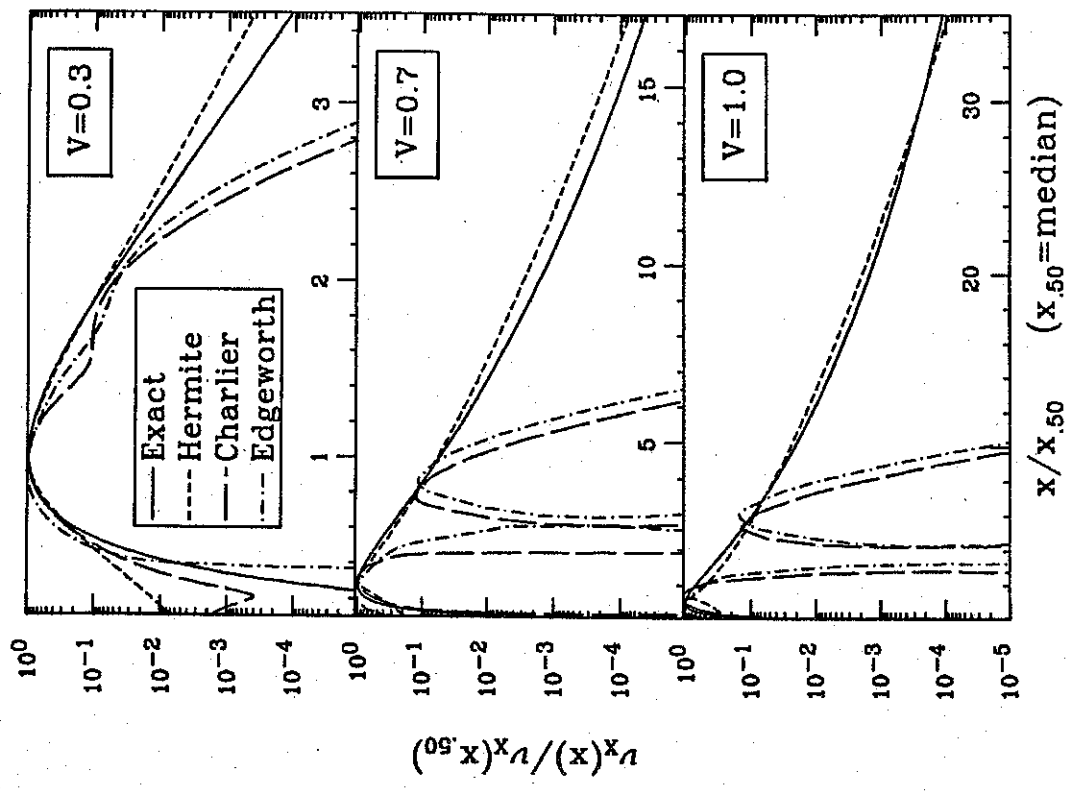


Fig. 3. Crossing rate estimates for lognormal responses.

Explicit Hermite Models of Hardening Responses.— In general, the Hermite models use monotonic polynomial transformations that expand the tails of the response distribution. By applying this transformation to a Gaussian process as in Eq. 7, various types of softening behavior ($\alpha_4 > 3$) are accurately modelled. For hardening responses with narrower tails, the polynomial transformation may instead be applied to the actual response, $X_0(t)$, to widen its tails to match the Gaussian model. If $O(h_n, h_n)$ terms are neglected in matching the moments of $U = g^{-1}(X_0)$ to those of the Gaussian model, a Hermite series for g^{-1} is similar to the softening series for g :

$$U(t) = g^{-1}(X_0(t)) = X_0(t) - \sum_{n=3}^N h_n He_{n-1}(X_0(t)) \quad (16)$$

This follows directly from Eqs. 7 and 13, noting that the approximations $X_0 \approx U + \sum h_n He_{n-1}(U) \approx U + \sum h_n He_{n-1}(X_0)$ are exact to first order in the Hermite moments h_n .

Unlike the softening Hermite model in Eq. 7, Eq. 16 yields an explicit Hermite series for the equivalent Gaussian fractile, $u = g^{-1}(x_0)$. As in the first-order softening model, the hardening model in Eq. 16 uses the actual Hermite moments h_n to scale non-Gaussian correction terms. These scaling factors can be modified, as in Eqs. 14-15, to include higher-order contributions to response moments. Such modifications, however, are (1) perhaps less necessary, because the first-order model in Eq. 16 does not appear to share the systematic bias of the first-order softening model; and (2) generally hindered by the need for additional moments of $X_0(t)$ to better calculate moments of Eq. 16. (These moment calculations are simplified if the Hermite polynomials in Eq. 16 are replaced by polynomials that are orthogonal with respect to $X_0(t)$; Appendix A shows how N such polynomials can be constructed from the first $2N-1$ moments of $X_0(t)$.)

Eq. 16 will be monotone if

$$\frac{dU}{dx_0} = 1 - \sum_{n=3}^N (n-1)h_n He_{n-2}(x_0) > 0 \quad (17a)$$

for all x_0 . If $N=4$, an equivalent condition in terms of response skewness and kurtosis is

$$16\alpha_3^2 < 9(3-\alpha_4)(5+\alpha_4) \quad (17b)$$

Fig. 1 shows that this monotone condition holds for most hardening ($\alpha_4 < 3$) responses, including all symmetric ($\alpha_3=0$) cases. In comparison with the classical Charlier/Edgeworth models, the combination of these Hermite hardening models (Eq. 16) and the second-order Hermite softening models (Eqs. 7 and 15)

can represent a far greater range of (α_3, α_4) values.

If Eq. 16 is monotone, Hermite response statistics analogous to Eqs. 9-11 are now in explicit form:

$$\nu_X(x) = \nu_0 \exp\left\{-\frac{1}{2}\left[x_0 - \sum_{n=3}^N h_n H e_{n-1}(x_0)\right]^2\right\} \quad (18)$$

$$F_X(x) = \Phi(x_0 - \sum_{n=3}^N h_n H e_{n-1}(x_0)) \quad (19)$$

$$f_X(x) \cdot \alpha_X = \varphi(x_0 - \sum_{n=3}^N h_n H e_{n-1}(x_0)) \left[1 - \sum_{n=3}^N (n-1) h_n H e_{n-2}(x_0)\right] \quad (20)$$

Fig. 4 compares Hermite estimates of $\nu_X(x)$ from Eq. 18 with exact results for various transformed Gaussian processes. Because all results except the Charlier series satisfy the dynamic assumption in Eq. 1b, deviations in Fig. 4 reflect differences in their static distributions. Based on this limited sample, these first-order Hermite estimates do not appear to share the systematic bias of the first-order softening Hermite model. Because their results generally fall within the scatter among various exact results with the same first 4 moments, these Hermite models are deemed adequate. In contrast, the Charlier (Edgeworth) estimates of $\nu_X(x)$ and $f_X(x)$ become negative in these cases when x exceeds roughly $3.5\sigma_X$ (not shown on the semilog scale in Fig. 4):

Application to Nonlinear Oscillators.— Consider the displacement response, $X(t)$, of an oscillator with nonlinear stiffness:

$$m\ddot{X}(t) + c\dot{X}(t) + K(X(t)) = F(t) \quad (21)$$

If the forcing function $F(t)$ has zero mean and constant spectral density S_0 , the theory of diffusion processes gives the exact results (Lyn, 1978):

$$\frac{\nu_X(x)}{\nu_X(0)} = \frac{f_X(x)}{f_X(0)} = \exp\left\{-\frac{U(x)}{k_0\sigma_0^2}\right\} \quad (22)$$

in terms of the initial stiffness $k_0 = K'(0)$, the initial variance $\sigma_0^2 = \pi S_0 / c k_0$, and the strain energy $U(x) = \int_0^x K(x) dx$. In the linear case, $U(x) = k_0 x^2 / 2$ and the Gaussian model is obtained.

Fig. 5 shows results for two forms of nonlinear stiffness -- a bilinear-elastic case and a continuously softening model. These models have the analytical forms shown on the figure, with parameters chosen to provide the kurtosis values displayed. (To maximize nonlinear effects in the bilinear case, the larger of the two yield levels producing the desired kurtosis has been used.) Fig. 5 also

shows four-moment estimates of $\nu_X(x)$ and $f_X(x)$ from the Charlier and Hermite series. These estimates of $\nu_X(x)/\nu_X(0)$ are repeated from Fig. 2; the corresponding $f_X(x)/f_X(0)$ estimates are identical for the Charlier series (because of the dynamic assumption in Eq. 1a) and are obtained from Eqs. 11 and 15 for the Hermite model.

Hermite estimates of $f_X(x)/f_X(0)$ in Fig. 5 show all the aforementioned advantages over the Charlier results: less erratic behavior, generally better prediction of the trend shown by various models with the given moments, and greater flexibility to model markedly non-Gaussian tail behavior. Hermite estimates of $\nu_X(x)/\nu_X(0)$ do not predict the exact results in Fig. 5 as well as those in Fig. 2, because the dynamic assumption in Eq. 1b is no longer satisfied. Note, however, that the true dynamic behavior cannot be identified by central moments, and that the Hermite models defined here generally lead to more conservative estimates of $\nu_X(x)$ than the Charlier and Edgeworth models. Of course, these Hermite models can be altered to take advantage of additional dynamic information. For example, $\nu_X(x)$ can be estimated by combining the foregoing Hermite estimate of $f_X(x)$ with Eq. 1a, if this dynamic model is known to be more accurate than Eq. 1b. In addition, Appendix B shows how these Hermite estimates of ν_X can be modified to account for knowledge of joint moments of $X(t)$ and $\dot{X}(t)$, as well as for nonstationarity and time-varying thresholds.

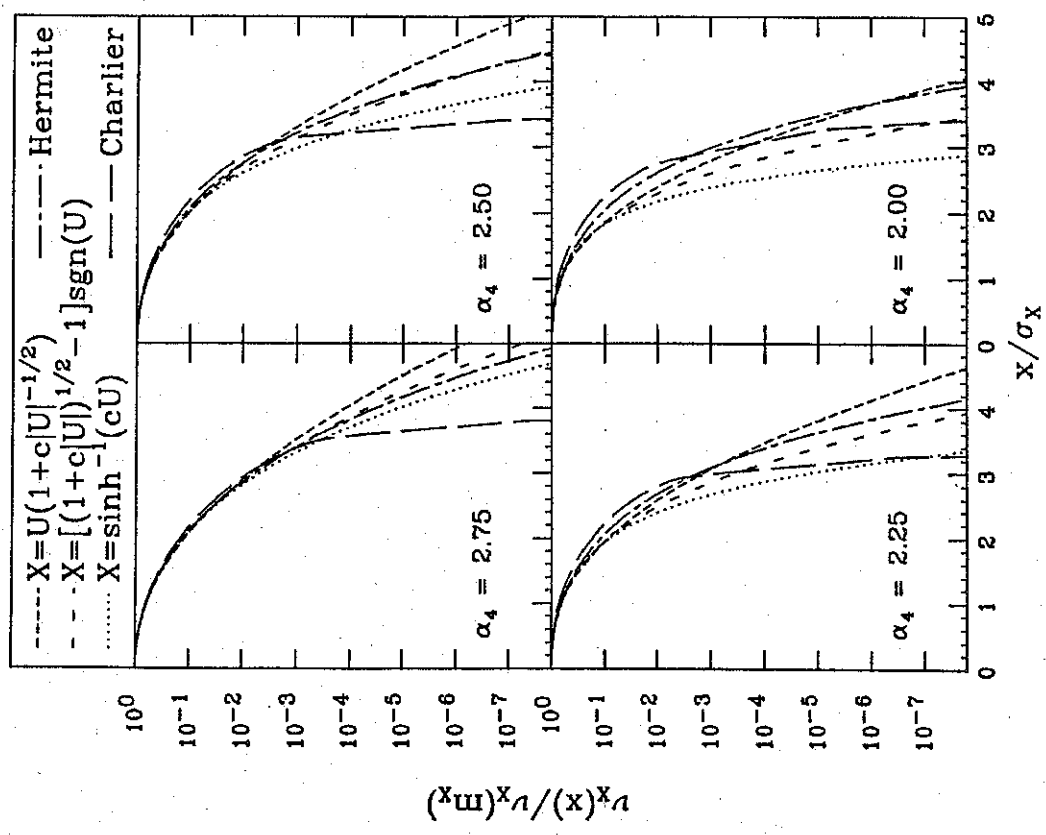


Fig. 4: Crossing rates for hardening transformations of normal processes.

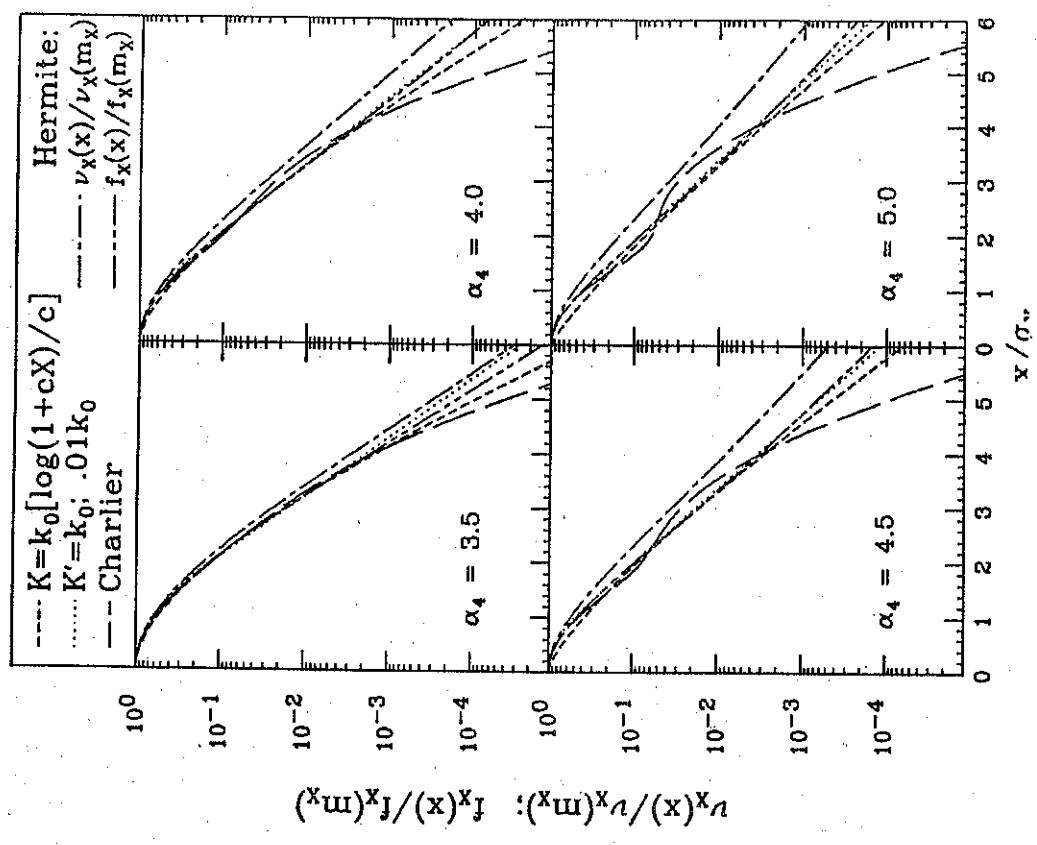


Fig. 5: Statistics of nonlinear oscillators.

SPECTRA, LOCAL AND GLOBAL EXTREMES, AND FATIGUE

Response Covariance and Spectral Density.— Because the various Hermite series terms in Eq. 7 form orthogonal processes, their second-moment properties are particularly simple. In terms of the correlation function $\rho_U(\tau)$ of $U(t)$, $E[He_n(U(t))He_m(U(t+\tau))]$ is given by $n![\rho_U(\tau)]^n$ if $n=m$ and zero otherwise. It follows that

$$\rho_X(\tau) = \kappa^2 \left\{ \rho_U(\tau) + \sum_{n=2}^N (n-1)! \tilde{h}_n^2 [\rho_U(\tau)]^{n-1} \right\} \quad (23)$$

$$S_X(\omega) = (\kappa\sigma_X)^2 \left\{ S_U(\omega) + \sum_{n=2}^N (n-1)! \tilde{h}_n^2 [S_U(\omega)]^{n-1} \right\} \quad (24)$$

(Eq. 14b ensures that $\rho_X(0)=1$). In the latter result, $S_U(\omega)$ and $S_X(\omega)$ are the spectral densities of $U(t)$ and $X(t)$, and $[S_U(\omega)]_n$ represents the n th-fold convolution of $S_U(\omega)$. Significantly, while differences between marginal moments of $X(t)$ and $U(t)$ are of first order in \tilde{h}_n , their spectra differ by only second-order terms. Hence the functional transformation can substantially alter the static distribution of a normal process without greatly changing its correlation structure. (Note that an arbitrary function g can be represented by a Hermite series with $N \rightarrow \infty$, so that these results apply to any function of a normal process.)

A useful spectral model for the underlying Gaussian process is

$$S_U(\omega; \omega_0, \delta) = \frac{1}{2} \left\{ \varphi \left(\frac{\omega - \omega_0}{\delta \omega_0} \right) + \varphi \left(\frac{\omega + \omega_0}{\delta \omega_0} \right) \right\} \quad (25)$$

in which ω_0 and δ reflect the central frequency and bandwidth of $U(t)$. The corresponding nonlinear spectrum in Eq. 24 becomes

$$S_X(\omega) = (\kappa\sigma_X)^2 \left\{ S_U(\omega; \omega_0, \delta) + 2\tilde{h}_2^2 \left[\frac{1}{2} S_U(\omega; 0, \sqrt{2}\delta) + \frac{1}{2} S_U(\omega; 2\omega_0, \sqrt{2}\delta) \right] + 6\tilde{h}_4^2 \left[\frac{3}{4} S_U(\omega; \omega_0, \sqrt{3}\delta) + \frac{1}{4} S_U(\omega; 3\omega_0, \sqrt{3}\delta) \right] + \dots \right\} \quad (26)$$

This shows the magnitudes of sub- and super-harmonics induced by the nonlinearity. Again, in comparison to changes in marginal distributions and moments, this redistribution of power is a second-order effect.

Global Extrema and First-Passage Failures.— For first-passage failures (e.g., first yield), it is useful to obtain statistics of the extreme value

$$E = \max\{X^n(t)\}^{1/n}, \quad 0 \leq t \leq T \quad (n=1, 2) \quad (27)$$

Thus, E is the maximum value of $X(t)$ if $n=1$ or of $|X(t)|$ if $n=2$, of interest in first passage beyond one- and two-sided barriers. If g is monotone, the conven-

tional Poisson model for upcrossings gives

$$P[E \leq x] = \exp\{-n\nu_0 T \exp(-\frac{x^2}{2})\} \quad (28)$$

in which the Gaussian fractile $u = g^{-1}((x - m_X)/\sigma_X)$ is given explicitly by Eq. 16 for hardening Hermite models, and implicitly by Eq. 7 for softening Hermite series. The softening model also yields explicit results for the fractile e_p such that $P[E \leq e_p] = p$:

$$e_p = m_X + \kappa\sigma_X \left\{ \nu_p + \sum_{n=2}^N \tilde{h}_n H e_{n-1}(\nu_p) \right\} \quad (29)$$

in which ν_p is the corresponding fractile of Gaussian extreme values; e.g., $\nu_p^2 = 2 \ln[n\nu_0 T / \ln(p^{-1})]$ for the Poisson model.

Eq. 28 can be refined to account for response bandwidth and clustering effects (*Winterstein and Cornell, 1985*):

$$P[E \leq x] = \exp\left\{-n\nu_0 T \exp\left(-\frac{x^2}{2}\right) \left[1 - 2\Phi\left(-\sqrt{\frac{\pi}{n}}u\right)\right]\right\} \quad (30a)$$

for a resonant response with damping ratio ζ . For an arbitrary spectral density estimate (e.g., from Fourier amplitudes of a time history), an "equivalent" damping ratio can be estimated as

$$\zeta = \left[8\nu_0 \pi^2 \int_{-\infty}^{+\infty} S_X^2(\omega) d\omega \right]^{-1} \quad (30b)$$

in which $S_X(\omega) = S_X(\omega)/\sigma_X^2$. This choice of ζ preserves the energy correlation time or "fluctuation scale," θ_g , which is roughly $(2\pi\nu_0)^{-1}$ for a lightly damped oscillator (*Winterstein and Cornell, 1985*). In comparison to estimates based on spectral moments, Eq. 30b is less sensitive to little-known high-frequency response behavior.

Local Response Extrema.— If g is monotone, maxima of $U(t)$ and $X(t) = g(U(t))$ occur at the same mean rate, ν_m . It is convenient to introduce the bandwidth measure $\epsilon = \sqrt{\nu_m^2 - \nu_0^2}/\nu_m$, which decreases from a maximum value of unity toward zero as the response bandwidth decreases and ν_m approaches ν_0 . Note that ϵ remains unchanged by the functional transformation, and that $\epsilon \approx 2\delta$ for the spectral model in Eqs. 25-26 if $\delta \ll 1$. The probability distributions of maxima and minima of $X(t)$, M_X^+ and M_X^- respectively, satisfy

$$P[M_X^+ \geq x] = \pm \alpha \epsilon^{-u^2/2} \Phi\left(\pm \frac{\alpha u}{\epsilon}\right) + \Phi\left(-\frac{u}{\epsilon}\right) \quad (-\infty < x < +\infty) \quad (31)$$

$$f_{M_X^+}(x) \cdot \sigma_X = \left[\pm \alpha u \epsilon^{-u^2/2} \Phi\left(\pm \frac{\alpha u}{\epsilon}\right) + \epsilon \varphi\left(\frac{u}{\epsilon}\right) \right] \frac{du}{dx_0}$$

in which $\alpha = \sqrt{1 - \epsilon^2}$ and " \pm " should be replaced by "+" for maxima and "-" for minima. As before, u is given by Eq. 7 or 16, and dx/dx_0 by Eq. 8a or 17a, depending on whether the softening or hardening Hermite model is used.

As in previous cases, the softening series give explicit results for fractiles of extrema. Because $P[M_X^* \geq x] \approx \alpha \exp(-u^2/2)$ for large x , upper fractiles of M_X^+ may be estimated by Eq. 12b, replacing p in its right side by p/α . The softening series also relate moments of M_X^+ explicitly to those of the corresponding Gaussian extrema, M_U^+ . Ignoring $O(\tilde{h}_n, \tilde{h}_m)$ terms,

$$E[(M_X^+)^b] = (\kappa\sigma_X)^b \left\{ E[(M_U^+)^b] + b \sum_{n=3}^N \tilde{h}_n E[(M_U^+)^{b-1} H_{e_{n-1}}(M_U^+)] \right\} \quad (32)$$

Eqs. 31-32 may be useful in predicting crack growth, which is typically governed by the maximum stress per cycle (generally with respect to a crack-opening stress level).

Response Envelopes and Ranges.— Fatigue damage is often related to response ranges, which in turn are conveniently studied through envelope behavior. Envelopes that pass near extrema of $X(t) = g(U(t))$ may be defined by applying the same function, g , to similar envelopes of Gaussian extrema:

$$M_U^\pm(t) = g(M_U^\pm(t)); \quad M_U^\pm(t) = U_s(t) \pm S_p(t) \quad (33)$$

Again, the positive and negative signs pertain to maxima and minima, respectively. The "slow" process, $U_s(t)$, is obtained by passing $U(t)$ through a linear lowpass filter, and $S_p(t)$ is an appropriate envelope of the remaining ("fast") process, $U_f(t) = U(t) - U_s(t)$. If $U_s(t)$ and $U_f(t)$ have contributions from relatively different frequency ranges, the partial envelope $S_p(t)$ is often more meaningful (i.e., more slowly varying) than the total envelope of $U(t)$. Significantly, while the choice of lowpass filter and envelope definition affects the dynamic behavior of $M_X^\pm(t)$ in Eq. 33, its marginal distribution satisfies Eq. 31 provided only that

- $Var[U_s] = \epsilon^2$, so that the slow and fast processes comprise the fractions ϵ^2 and α^2 of the total variance; and
- $U_s(t)$ and $S_p(t)$ are independent.

Various choices of $U_s(t)$ and $S_p(t)$ satisfy these conditions, with the usual tradeoffs between envelopes that follow all extrema (Madsen et al, 1986) and those with more stable dynamic behavior (Van Dyck, 1961). The extremal envelopes in Eq. 33 are particularly useful if $U(t)$ has bimodal spectrum, with $U_s(t)$ effectively the response of the low-frequency "mode" (Toro and Cornell, 1986).

The difference between the envelopes of maxima and minima gives a useful model of response ranges:

$$R \approx M_X^+ - M_X^- = g(U_s + S_p) - g(U_s - S_p) \quad (34a)$$

$$\begin{aligned} &= \kappa\sigma_X \{ 2S_p + \sum_{n=3}^N \tilde{h}_n [H_{e_{n-1}}(U_s + S_p) - H_{e_{n-1}}(U_s - S_p)] \} \\ &= 2\kappa\sigma_X \{ S_p + \tilde{h}_3(2U_s S_p) + \tilde{h}_4(S_p^3 - 3S_p(1 - U_s^2)) + \dots \} \end{aligned} \quad (34b)$$

Eq. 34b estimates g from the softening Hermite model (Eq. 7). In the Gaussian case ($\tilde{h}_n = 0$ and $\kappa = 1$), Eq. 34 yields $R = 2\sigma_X S_p$ so that $P[R > r]$ is given by $\exp[-r^2/2(\alpha\sigma_X)^2]$. This Rayleigh model, which scales narrow-band ranges down by a factor of α to reflect bandwidth effects, gives the exact mean value and agrees well with simulated ranges of relatively broad-band processes (Winterstein, 1984).

In general, the range model above includes the effects of both response bandwidth (through α and ϵ) and nonlinearity (through the Hermite moments \tilde{h}_n). For example, the range moment $E[R^b]$ is given by $(2\sqrt{2}\sigma_X)^b (b/2)!$ for narrow-band Gaussian responses; the four-moment Hermite model corrects this value for bandwidth and nonlinear effects as follows:

$$\frac{E[R^b]}{(2\sqrt{2}\sigma_X)^b (b/2)!} = (\alpha\epsilon)^b \{ 1 + b(b-1) [\alpha^2 \tilde{h}_4 + 2\epsilon^2 \tilde{h}_3^2 + (\frac{\alpha^4}{2} (b^2 + 5) + 9\epsilon^4) \tilde{h}_4^2] \} \quad (35)$$

Consistent with previous results, Eq. 35 retains only first- and second-order terms in the coefficients \tilde{h}_n . This result is particularly useful in fatigue applications, as shown below.

Fatigue Damage Rates.— If the stress response $X(t)$ is sufficiently narrow-band, it is common to relate growth in fatigue damage, $D(t)$, to ranges of $X(t)$. Specifically, assume that a stress range R causes incremental damage $\Delta D = cR^b$ regardless of past load history; this includes Miner's law as well as crack growth models that are separable functions of stress and crack size (Winterstein, 1984). If $X(t)$ is narrow-band and Gaussian, the mean damage is $c \nu_0 t (2\sqrt{2}\sigma_X)^b (b/2)!$. Deviations from this result are conveniently introduced through a unitless correction factor γ , which can be evaluated from Eq. 35 with $\alpha \rightarrow 1$ ($\epsilon \rightarrow 0$) for narrow-band responses. If the first-order softening Hermite model is used (and hence only first-order terms in Eq. 35 are kept), the resulting γ estimate is particularly simple:

$$\gamma = \frac{E[D(t)]}{c \nu_0 t (2\sqrt{2}\sigma_X)^b (b/2)!} = 1 + b(b-1) h_4 \quad (36)$$

based on the Hermite moment $h_4 = (\alpha_4 - 3)/24$.

Eq. 36 was previously reported by Winterstein (1985), where it was shown to accurately predict the rainfall damage simulations reported by Lutes et al (1984) for $2 \leq b \leq 5$. Because of its first-order nature, however, errors in Eq. 36 may become more significant for larger values of b (or greater nonlinearities). Including second-order terms from Eq. 35 may improve γ estimates for moderate b values, but its neglect of higher-order terms may produce consistently low damage estimates for higher exponents. Its second-order expansion of R^b does provide a useful second-moment range description, however — in the narrow-band case,

$$m_R = E[R] = \sqrt{2\pi} \kappa \sigma_X \tag{37}$$

$$V_R^2 = \frac{\sigma_R^2}{m_R^2} = \frac{4}{\pi} (1 + h_4 + \tilde{h}_4) - 1$$

(The relation $h_4 = \tilde{h}_4 + 9\tilde{h}_4^2$, which follows from Eq. 15, has been used to eliminate \tilde{h}_4^2 .) For linear responses, $\kappa=1$ and $h_4 = \tilde{h}_4 = 0$ so that Eq. 37 gives $V_R = 5.23$, consistent with the Rayleigh distribution.

Instead of estimating higher range moments directly from Eq. 35, these (more reliable) second-moment statistics are used to fit a Weibull model to nonlinear stress ranges. While this model's parameters and higher moments are given only implicitly by its second-moment statistics, $E[R^b]$ can be explicitly approximated (Cornell and Winterstein, 1986) by $(m_R/V_R)^b (b V_R)!$ (with good accuracy if $V_R \leq 1$, which includes most cases of interest). Dividing this estimate of $E[R^b]$ by the corresponding Gaussian result, the correction factor γ is found to be

$$\gamma = \left[\frac{\sqrt{\pi} \kappa}{2 V_R} \right]^b \frac{(b V_R)!}{(b/2)!} \tag{38}$$

with V_R determined from Eq. 37. This result overestimates the exact value ($\gamma=1$) in the linear case, due to the approximate fit of the Weibull distribution. Compared to the first-order estimate (Eq. 36), the second-order estimate of γ in Eq. 38 is shown below to more accurately predict fatigue due to wave loads for large values of b and α_4 .

Eq. 36 or 38 may be combined with a second correction factor to reflect bandwidth effects on mean damage obtained by rainfall counting (e.g., *Wirsching and Light, 1980; Winterstein, 1984, 1985*). Note, however, that this second factor generally decreases with bandwidth for Gaussian processes (*Wirsching and Light, 1980; Madsen et al, 1986*), and hence also for their monotonic transformations. Thus the narrow-band assumption in Eq. 36, which avoids the

need for bandwidth information, may typically be conservative with respect to the rainfall-counting assumption.

HERMITE MODELS OF MORISON WAVE FORCES

One source of nonlinearity in offshore structures arises from nonlinear fluid drag forces. These forces are typically combined with inertial effects through the formula of Morison (1950), which gives the force per unit length on a fixed cylinder:

$$F(t) = k_m \dot{V}(t) + k_d V(t) |V(t)| \tag{41}$$

in terms of the wave particle velocity, $V(t)$, and the drag and mass coefficients, k_d and k_m . For conventional structures in moderate water depths, stresses are often assumed proportional to the wave force in Eq. 41 (i.e., quasi-static behavior). It is further assumed that the random process $V(t)$ is (1) Gaussian, (2) mean-zero, and (3) stationary. The first assumption is consistent with linear wave theory, the second applies in the absence of current, and the third is appropriate over a time scale of several hours (within a particular "sea-state"). These assumptions are readily generalized through a moment-based Hermite model of $V(t)$ based on observed wave statistics.

It is convenient to consider the normalized force (and quasi-static response), $X(t) = F(t)/k_m \sigma_V$. Exact calculation of $\nu_X(x)$ requires numerical integration, as well as knowledge of the regularity factor, α , of $V(t)$. As the bandwidth of $V(t)$ decreases, however, a simple asymptotic result is available (Madsen et al, 1986):

$$\frac{\nu_X(x)}{\nu_0} = \begin{cases} \exp(-\frac{x^2}{2}) & |x| < \frac{1}{2d} \\ \exp(-\frac{1}{2d} |x - \frac{1}{4d}|) & |x| \geq \frac{1}{2d} \end{cases} \tag{42}$$

based on the unitless drag parameter, $d = k_d \sigma_V^2 / k_m \sigma_V$. For example, $d = C_d \sigma_V / C_m \pi^2 D \nu_0$ for a circular cylinder of diameter D , reflecting that nonlinear drag contributions will increase as either the pile diameter or mean wave frequency is reduced. The value of d is related directly to the fourth moment of $X(t)$:

$$h_4 = \frac{\alpha_4 - 3}{24} = 3.25 \left(\frac{d^2}{1 + 3d^2} \right)^2 \tag{43}$$

Thus h_4 directly reflects the degree of nonlinearity, growing with d from zero to a maximum value of .361 ($\alpha_4 = 11.7$). As $d \rightarrow 0$, inertial effects dominate and both

the "exact" result (Eq. 42) and the Hermite estimate approach the linear (Gaussian) model.

Fig. 6 shows estimates of the median extreme value of $X(t)$, $e_{.05}$, over varying durations, T . (Due to the Poisson assumption, these are also median extreme estimates for $|X(t)|$ over durations $T/2$.) The "exact" curves satisfy $\exp[-\nu\chi(e_{.05}T)]=0.5$, with $\nu\chi(x)$ from Eq. 42. Corresponding Hermite estimates of $e_{.05}$ follow Eq. 29:

$$e_{.05} = \kappa \sqrt{1+3d^2} [u_{.05} + \tilde{h}_4(u_{.05}^3 - 3u_{.05})] \quad (44)$$

in terms of the median extreme for a standard Gaussian; e.g., $u_{.05} = [2\ln(1.44\nu_0 T)]^{1/2}$. The first-order Hermite result replaces \tilde{h}_4 by h_4 and κ by unity (Eq. 13), while the second-order estimate bases \tilde{h}_4 and κ on h_4 as in Eq. 15. Two Gaussian results are also formed by replacing $V|V|$ with a linear term of the form $\beta\sigma_V V$. The curves shown use the values $\beta = \sqrt{3} = 1.73$, which preserves the variance of $X(t)$, and $\beta = \sqrt{3}/\pi = 1.60$, the standard choice from equivalent linearization. Resulting values of $e_{.05}$ can be obtained from Eq. 44, replacing $3d^2$ by $(\beta d)^2$, κ by 1, and \tilde{h}_4 by 0.

Because the fractile $e_{.05}$ is normalized in Fig. 6 with respect to the correct response variance $\sigma_X^2 = 1+3d^2$, the Gaussian model with correct variance yields a result independent of d . The corresponding result from equivalent linearization decreases with d , because it underestimates the response variance. If d exceeds roughly .2-.4, both Gaussian results become increasingly unconservative as either d or T grows. In contrast, the first-order Hermite estimate is generally conservative, because its variance and kurtosis are larger than those of the actual response. The second-order Hermite result provides a substantial improvement, with good accuracy even in strongly nonlinear, drag-dominated cases.

Fig. 7 shows estimates of fatigue correction factors, γ , for quasi-static Morison responses with various stress exponents. The exact result calculates $E[R^b]$ by numerically integrating $(2x)^b |\nu'x(x)|/\nu_0$ over positive x values (Madsen et al., 1986). A simpler closed-form result is also shown, based on decoupling the effects of drag and inertia (Winterstein, 1984):

$$\gamma = \frac{1 + \frac{b!}{(b/2)!} (\sqrt{2d})^b}{[1 + 3d^2]^{b/2}} \quad (45)$$

Eq. 45 follows the exact result accurately over the entire range of d values. Among the approximate moment-based estimates of γ , the second-order Hermite results are found superior to the first-order estimates if d exceeds roughly 0.3, with marked improvement over the first-order result for large b values.

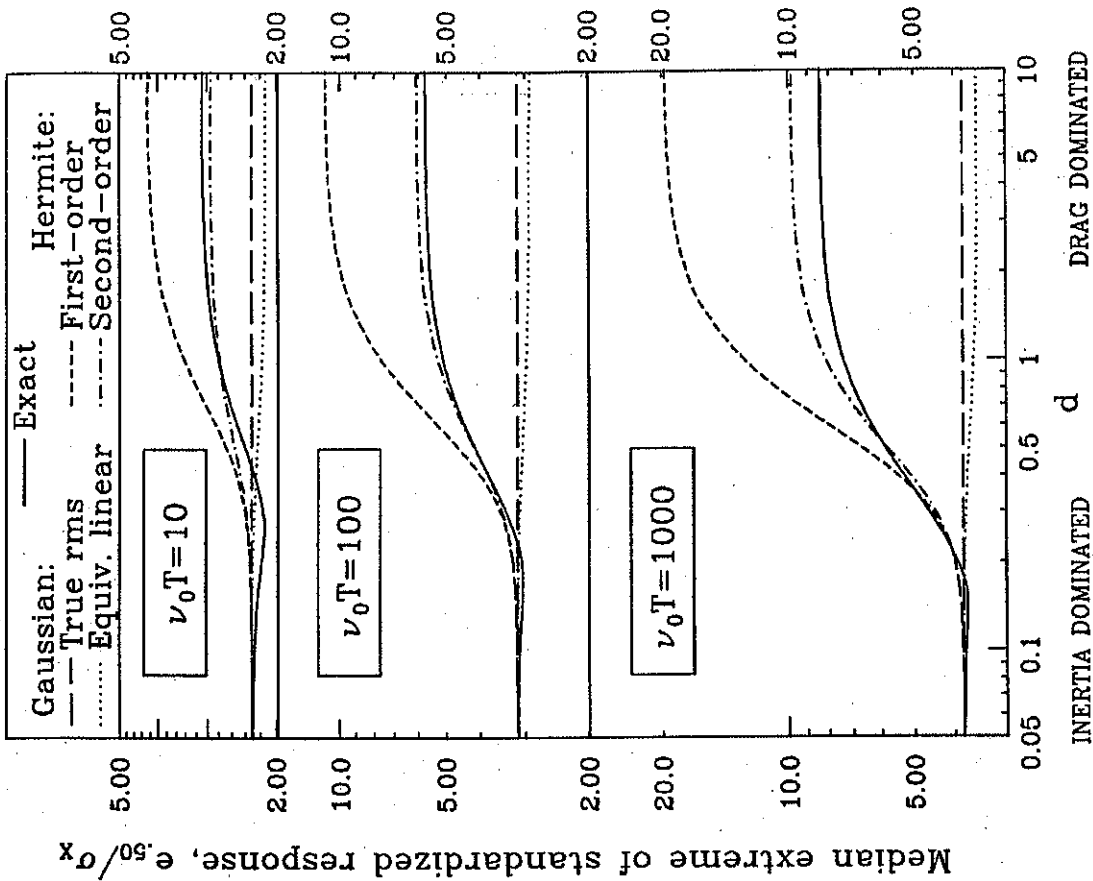


Fig. 6: Extremes of Morison wave loads.

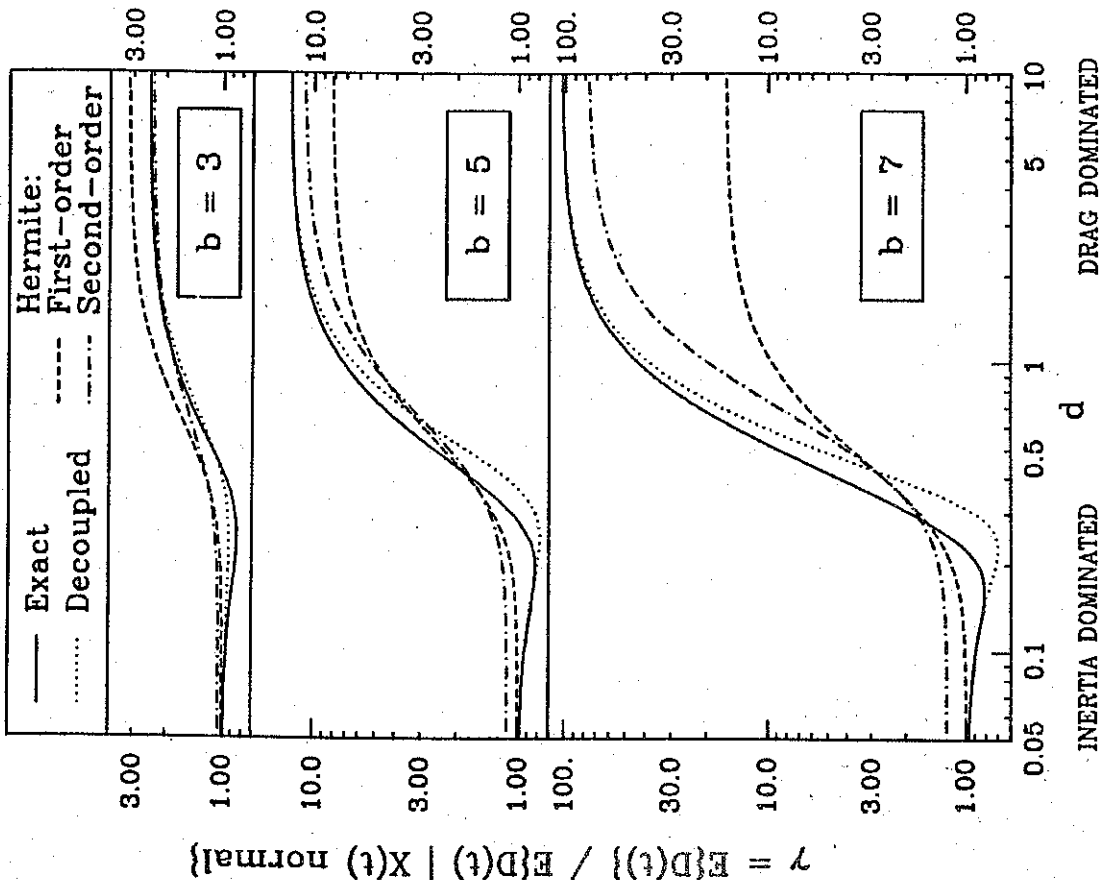


Fig. 7. Fatigue under Morison wave loads.

SUMMARY AND CONCLUSIONS

Traditional Charlier and Edgeworth series for random variables have been generalized to provide first-order densities and crossing statistics of dynamic responses (Eqs. 1a and 6). When these series are based on a moderate number of moments, however, they may not accurately reflect significant nonlinearities. Results may be multi-modal or even negative; e.g., four-moment Charlier and Edgeworth estimates of $f_X(x)$ and $v_X(x)$ become negative for all hardening ($\alpha_4 < 3$) responses. The extent of softening ($\alpha_4 > 3$) and asymmetry that can be modelled acceptably is also limited (Fig. 1).

Alternative dynamic models have been formulated here through moment-based Hermite series. With these series, the necessary response statistics for extremes and fatigue can be predicted from response moments, which are generally simpler to estimate (from either time histories or analytical models). These models assume that $X(t) = g(U(t))$, in terms of a Gaussian response $U(t)$. This assumption leads to a particularly tractable model, reducing nonlinear analysis in many cases to simple transformation of well-known results for linear (Gaussian) responses.

Hermite series estimates of g and g^{-1} are derived for softening and hardening responses, respectively (Eqs. 7 and 16). "First-order" models, which match response moments to first-order in non-Gaussian contributions, utilize the same coefficients ("Hermite moments") as the Charlier series. These Hermite models are found to be considerably more flexible, however, avoiding the possibility of negative probability densities and crossing rates. The first-order softening model has also been extended to include second-order nonlinear contributions, permitting more accurate softening models through simple modification of series coefficients (e.g., Eq. 15). These second-order models are shown to give more accurate estimates of crossing rates (Fig. 2), extremes (Fig. 6), and fatigue (Fig. 7). The latter two results illustrate the use of Hermite models of Morison wave forces and quasi-static responses. Good agreement has also been demonstrated for statistics of nonlinear oscillators (Fig. 5).

ACKNOWLEDGEMENTS

Portions of this research were carried out while the author was a visiting researcher at the Technical University of Denmark; it is a pleasure to acknowledge the helpful discussions and hospitality of Ove Ditlevsen, Peter Bjerager, and Steen Krenk extended to the author during his stay. This material is also based in part upon work supported by the National Science Foundation under Grant No. CEE-8410845.

REFERENCES

Charlier, C.V.L. (1906). "Über die Darstellung willkürlicher Funktionen," *Arkiv for Matematik, Astronomi och Fysik*, Vol. 2, No. 20, 1905, pp. 1-35.

Cornell, C.A. and Winterstein, S.R. (1986). "Applicability of the Poisson Earthquake-Occurrence Model," *EPRF Report NP-4770*, Research Project P101-38, Electric Power Research Institute, Aug., 1986.

Crandall, S.H. (1980). "Non-Gaussian Closure for Random Vibration of Non-Linear Oscillators," *International Journal of Non-Linear Mechanics*, Vol. 15, 1980, pp. 303-313.

Davenport, A.G. (1964). "Note on the Distribution of the Largest Value of a Random Function with Application in Gust Loading," *Proceedings of the Institution of Civil Engineers*, London, England, Vol. 28, 1964, pp. 187-196.

Edgeworth, F.Y. (1907). "On the Representation of Statistical Frequency by a Series," *Journal of the Royal Statistical Society, Series A*, Vol. 70, 1907, pp. 102-106.

Grigoriu, M. (1984a). "Crossings of Non-Gaussian Translation Processes," *Journal of Engineering Mechanics*, ASCE, Vol. 110, No. 4, Apr., 1984, pp. 610-620.

Grigoriu, M. (1984b). "Extremes of Wave Forces," *Journal of Engineering Mechanics*, ASCE, Vol. 110, No. 12, Dec., 1984, pp. 1731-1742.

Johnson, N.L., and Kotz, S. (1970). *Continuous Univariate Distributions - I*, John Wiley & Sons, Inc., New York, N.Y., 1970.

Lin, Y.K. (1976). *Probabilistic Theory of Structural Dynamics*, Robert E. Krieger Publishing Company, Huntington, N.Y., 1976.

Lutes, L.D., Corrao, M., Hu, S.J., and Zimmerman, J. (1984). "Stochastic Fatigue Damage Analysis," *Journal of Structural Engineering*, ASCE, Vol. 110, No. 11, Nov., 1984, pp. 2585-2601.

Lutes, L.D., and Hu, S.J. (1986). "Non-Normal Stochastic Response of Linear Systems," *Journal of Engineering Mechanics*, ASCE, Vol. 112, No. 2, Feb., 1986, pp. 127-141.

Madsen, H., Krenk, S., and Lind, N.C. (1986). *Methods of Structural Safety*, Prentice-Hall, Inc., Englewood Cliffs, N.J., 1986.

Morison, J.R., O'Brien, M.P., Johnson, J.W., and Shaaf, S.A. (1950). "The Force Exerted by Surface Waves on Piles," *Petroleum Transactions*, AIME, Vol. 189, 1950, pp. 149-154.

Murotsu, Y., Okada, H., Kishi, M., Yonezawa, M., and Niwa, K. (1981). "Fourth-Order Moment Approximation to Reliability of Non-linear Structure," *Transactions of the Sixth International Conference on Structural Mechanics in Reactor Technology*, Paper No. M12, Paris, France, Aug. 17-21, 1981.

Ochi, M.K. (1986). "Non-Gaussian Random Processes in Ocean Engineering," *Probabilistic Engineering Mechanics*, Vol. 1, No. 1, 1986, pp. 28-39.

Rice, S.O. (1944). "Mathematical Analysis of Random Noise," *Bell Technical Journal*, Vol. 23, 1944, and Vol. 24, 1945; reprinted in *Selected Papers on Noise and Stochastic Processes*, Wax, ed., Dover, 1952.

Schetzen, M. (1980). *The Volterra and Wiener Theories of Nonlinear Systems*, John Wiley & Sons, Inc., New York, N.Y., 1980.

Soize, C. (1978). "Gust Loading Factors with Nonlinear Pressure Terms," *Journal of the Structural Division*, ASCE, Vol. 104, No. ST6, Jun., 1978, pp. 991-1007.

Stratonovich, R.L. (1963). *Topics in the Theory of Random Noise*, Vols. I and II, Gordon and Breach, New York, 1963.

Toro, G.R., and Cornell, C.A. (1986). "Extremes of Gaussian Processes with Hirmodal Spectra," *Journal of Engineering Mechanics*, Vol. 112, No. 5, May, 1986, pp. 465-484.

Van Dyck, J.F.M. (1981). "Envelopes of Broad Band Processes," thesis presented to the Massachusetts Institute of Technology, at Cambridge, Mass., June, 1981, in partial fulfillment of the requirements for the degree of Master of Science.

Winterstein, S.R. (1984). "Diffusion Models and the Energy Fluctuation Scale: A Unified Approach to Extremes and Fatigue," *Technical Report No. 64*, John A. Blume Earthquake Engineering Center, Stanford University, Nov., 1984.

Winterstein, S.R., and Cornell, C.A. (1985). "Energy Fluctuation Scale and Diffusion Models," *Journal of Engineering Mechanics*, ASCE, Vol. 111, No. 2, Feb., 1985, pp. 125-142.

Winterstein, S.R. (1985). "Non-Normal Responses and Fatigue Damage," *Journal of Engineering Mechanics*, ASCE, Vol. 111, No. 10, Oct., 1985, pp. 1291-1295.

Wirsching, P.H., and Light, M.C. (1980). "Fatigue under Wide Band Random Stresses," *Journal of the Structural Division*, ASCE, Vol. 106, No. ST7, July, 1980, pp. 1593-1607.

Wu, W.F., and Lin, Y.K. (1984). "Cumulant-Neglect Closure for Non-Linear Oscillators under Random Parametric and External Excitations," *International Journal of Non-Linear Mechanics*, Vol. 19, 1984, pp. 349-362.

Appendix A:

ORTHOGONAL EXPANSIONS FOR RANDOM PROCESSES

Various results for a random process $U(t)$ are conveniently expressed in terms of polynomials, $P_n[U(t)]$, that possess orthogonal properties:

$$E[P_n(U)] = E[P_n(U)P_m(U)] = 0 \quad (n \neq m; \quad n, m > 0) \quad (A1)$$

(The argument t is omitted for brevity.) The n th such polynomial can be constructed from the simple power law $U^n(t)$ by removing its correlation with all lower-order polynomials:

$$P_n(U) = U^n - \sum_{k=0}^{n-1} c_{nk} P_k(U); \quad c_{nk} = \frac{E[U^n P_k(U)]}{E[P_k^2(U)]} \quad (A2)$$

The orthogonality property in Eq. A1 is readily verified by induction. This procedure is analogous to the Gram-Schmidt method, in which a vector is made orthogonal by subtracting its projection onto all preceding vectors. Multivariate orthogonal polynomials can be constructed similarly, replacing U by $U = [U_1, \dots, U_p]$ and U^n by $U_1^{n_1} \dots U_p^{n_p}$.

If $U(t)$ has been standardized to have zero mean and unit variance, applying Eq. A2 with $P_0(U) = 1$ leads to the polynomials

$$\begin{aligned} P_1(U) &= U; \\ P_3(U) &= U^3 - c_{32} P_2(U) - c_{41} U - c_3; \end{aligned} \quad \dots \quad P_2(U) = U^2 - c_3 U - 1; \quad (A3)$$

in which $c_{32} = E[U^3 P_2(U)] / E[P_2^2(U)] = (\alpha_5 - \alpha_3 \alpha_3) / (\alpha_4 - \alpha_3^2 - 1)$. If $U(t)$ has not been standardized, the orthogonal property can be achieved by replacing U by $(U - m_U) / \sigma_U$ in Eq. A3. Note that in general, N orthogonal polynomials require knowledge of the first $2N - 1$ moments of $U(t)$, but not its full marginal distribution function. Also, because $E[P_2^2(U)] = \alpha_4 - \alpha_3^2 - 1$ cannot be negative, the kurtosis value α_4 cannot be less than $\alpha_3^2 + 1$ (Fig. 1).

Moment-Based Distribution Series. If $U(t)$ represents an analytical random process model (normal, lognormal, exponential, etc.), various generalizations of this model can be formed from series of these orthogonal polynomials. For example, suppose one wishes to model a new random process, $X(t)$, from only its first N moments. To judge the degree to which $X(t)$ varies from $U(t)$, these moments can be used to calculate the *orthogonal polynomial moments* P_n :

$$P_n = \frac{E[P_n(X)]}{E[P_n^2(U)]} \quad (A4)$$

The P_n values are linear combinations of the first n moments of $X(t)$. As the distribution of $X(t)$ approaches that of $U(t)$, Eq. A1 ensures that $P_n \rightarrow 0$ for all $n > 0$. More generally, the P_n values can be used to estimate the probability density of $X(t)$ from that of $U(t)$:

$$f_X(u) = \sum_{n=0}^N P_n P_n(u) \tag{A5}$$

This probability density reproduces the specified polynomial moments P_1, \dots, P_N (and hence the associated central moments), and sets higher polynomial moments to zero:

$$E[P_m(X)] = \int_{-\infty}^{+\infty} P_m(u) f_X(u) du = \sum_{n=0}^N P_n \int_{-\infty}^{+\infty} P_m(u) P_n(u) f_U(u) du = \begin{cases} P_m E[P_m^2(U)] & (0 \leq m \leq N) \\ 0 & (m > N) \end{cases} \tag{A6}$$

The latter equality, which follows from orthogonality (Eq. A1), shows that the moments P_0, \dots, P_N from Eq. A5 are consistent with those defined in Eq. A4. Taking $m=0$, this result confirms that Eq. A5 encloses unit area. While these results do not require that $X(t)$ be standardized, convergence of Eq. A5 is generally faster if $X(t)$ is scaled to have the same low-order moments as the "parent process" $U(t)$. If $X(t)$ and $U(t)$ are standardized, $P_1=P_2=0$ and Eq. A5 modifies the PDF of $U(t)$ to match third and higher moments of $X(t)$.

If $X(t)$ is the response of a mildly nonlinear system, a natural choice for the parent process $U(t)$ is the linear/Gaussian model. In this case $U(t)$ has central moments $\alpha_3=\alpha_5=0$ and $\alpha_4=3$, so that Eqs. A2-A3 reduce to the Hermite polynomials given after Eq. 2. Similarly, because $E[P_n^2(U)]=n!$ in this case, Eqs. A4 and A5 reduce to Eqs. 3 and 2, respectively. Other useful choices of $U(t)$ are gamma and beta processes, leading respectively to associated Laguerre and Jacobi polynomials. (In particular, an exponential process is a useful parent process for the squared "energy" envelope of nonlinear responses.)

A common drawback of these models is their lack of flexibility, arising from the use of a polynomial (Eq. A5) to approximate the ratio between the actual and parent PDFs, $f_X(u)/f_U(u)$. Unless many terms (moments) are retained, the resulting f_X estimate cannot deviate significantly from f_U , and significantly different moments often require an ill-behaved f_X ; e.g., multimodal and possibly negative (Fig. 1). More flexible behavior may be obtained by using these polynomial series to functionally transform the parent process, $U(t)$.

Functionally Transformed Processes. The statistics of a functionally transformed process, $X(t)=g(U(t))$, are also conveniently obtained by replacing g by a series of orthogonal polynomials:

$$X = g(U) = \sum_{n=0}^N g_n P_n(U) \tag{A7}$$

in which the coefficients g_n are given by

$$g_n = \frac{E[g(U)P_n(U)]}{E[P_n^2(U)]} \tag{A8}$$

Eq. A8 determines g_n from the orthogonality relations (Eq. A1), in the same way that calculation of Fourier coefficients utilizes the orthogonality of sinusoids with different frequencies. Several properties of Eqs. A7-A8 are noteworthy:

- As the number of terms grows, virtually any smooth function g can be represented with arbitrary accuracy.
- By truncating Eq. A7 at $n=N$, the result is the "best" N th-order polynomial approximation to g , in the sense that the mean-square error in approximating g is minimized. The result is hence equivalent to least-squares fit of an N th-order polynomial to $X=g(U)$, given infinite data (i.e., the entire population). Finite sample least-squares results can also be obtained from Eqs. A7-A8, by interpreting the expectations in Eqs. A2 and A8 as sample averages.

Second-moment properties of $X=g(U)$ are simply obtained in terms of g_n :

$$E[X(t)] = g_0 \\ \text{Var}[X(t)] = \sum_{n=2}^N g_n^2 E[P_n^2(U)] \tag{A9}$$

This summation often converges relatively quickly, i.e., g can be approximated by a low-order polynomial without greatly affecting its second-moment statistics. The covariance function of $X(t)=g(U(t))$ is generally a double summation in terms of $R_{mn}(\tau)=\text{Cov}[P_m(U(t)), P_n(U(t+\tau))]$:

$$R_X(\tau) = \text{Cov}[X(t), X(t+\tau)] = \sum_{m,n=0}^N g_m g_n R_{mn}(\tau) \tag{A10}$$

Because they often occur in practical applications, it is useful to specialize this result to cases in which the joint PDF of $U(t)$ and $U(t+\tau)$ is of the form

$$f(u_1, u_2, \tau) = f_U(u_1) f_U(u_2) \prod_{n=0}^{\infty} P_n(u_1) P_n(u_2) \frac{[\rho_U(\tau)]^n}{E[P_n^2(U)]} \tag{A11}$$

in which $\rho_U(\tau)$ is the correlation function of $U(t)$. (With $P_0=1$, Eq. A1 ensures that this result encloses unit volume and yields the marginal density f_U and

correlation function ρ_U . Eq. A11 holds for normal and chi-square-2 processes, for example, which are useful parent processes for nonlinear responses and their energy envelopes. In these cases, the P_n become Hermite and Laguerre polynomials (Table A-1), and $E[P_n^2(U)]$ equals $n!$ and $(n!)^2$, respectively. Eq. A11 implies that $P_m[U(t)]$ and $P_n[U(t)]$ are *orthogonal processes*, and that the correlation function of $P_n[U(t)]$ is $[\rho_U(\tau)]^n$.

$$R_{mn}(\tau) = \text{Cov}[P_m(U(t)), P_n(U(t+\tau))] = \begin{cases} E[P_n^2(U)] [\rho_U(\tau)]^n & n=m > 0 \\ 0 & \text{otherwise} \end{cases} \quad (\text{A12})$$

(Note that Eq. A12 is more general than Eq. A1, which ensures orthogonality only at $\tau=0$, so that $P_m[U(t)]$ and $P_n[U(t)]$ are orthogonal *random variables*.) Given Eq. A12, the covariance and spectral density functions of $X(t)=g(U(t))$ can be written in series form:

$$\begin{aligned} R_X(\tau) &= \sum_{n=1}^{\infty} g_n^2 E[P_n^2(U)] [\rho_U(\tau)]^n \\ S_X(\omega) &= \sum_{n=1}^{\infty} g_n^2 E[P_n^2(U)] [s_U(\omega)]^n \end{aligned} \quad (\text{A13})$$

In which $s_U(\omega)$ is the unit-area spectral density of $U(t)$, and $[s_U(\omega)]^n$ is its n -fold convolution. As in Eq. A9, the important (macro-scale, low frequency) statistics of $X(t)$ are often governed by the first few terms in these summations. If $U(t)$ is Gaussian, Eq. A13 reduces to Eqs. 23-24 in the main text.

Moment-based Functional Transformations. To overcome the limitations of moment-based distribution series shown above, it is useful to seek functional transformations such as Eq. A7 that preserve the first N moments of $X(t)$. It is convenient to consider a function g that relates the parent process $U(t)$ to a standardized response $X_0(t)=[X(t)-m_X]/\sigma_X$; in this case $g_0=0$ because $E[X_0]=0$ (Eq. A9). Rewriting Eq. A7 with $g_1=\kappa$ and $g_n/g_1=c_{n+1}$ for $n \geq 2$,

$$X_0 = \frac{X - m_X}{\sigma_X} = \kappa [P_1(U) + \sum_{n=3}^N c_n P_{n-1}(U)] \quad (\text{A14})$$

In which the scaling factor κ ensures that X_0 has correct (unit) variance, and the shape factors c_n scale nonlinear terms to preserve higher moments of $X(t)$. In view of Eq. A9, $\text{Var}[X_0]=1$ if

$$\kappa = \left[1 + \sum_{n=3}^N c_n^2 E[P_{n-1}^2(U)] \right]^{-1/2} \quad (\text{A15})$$

Eqs. A14-A15 generalizes the results of Eqs. 7 and 14 to include non-Gaussian $U(t)$.

Series Calibration: Second-order Hermite Series Results. It remains to calibrate nonlinear contributions to Eq. A14; i.e., determine coefficients c_3, \dots, c_N that provide specified orthogonal polynomial moments P_3, \dots, P_N of $X_0=g(U)$. This leads to a set of simultaneous nonlinear equations for the coefficients c_n , whose solution (if any) is difficult to obtain. Because these coefficients c_n are often less than unity (if an appropriate parent process is chosen), we simplify this calibration by retaining only first- and second-order terms in c_n in calculating response moments. It is also convenient to specialize Eq. A14 to Gaussian $U(t)$, for which the P_n become Hermite polynomials, with moments

$$E[He_n(X_0)] \approx E[He_n(X_0/\kappa)] \quad (\text{A16})$$

$$\approx E[He_n(U)] + E[He_n'(U)] (X_0/\kappa - U)$$

$$+ \frac{1}{2} E[He_n''(U)] (X_0/\kappa - U)^2$$

$$= E[He_n(U)] + n \sum_{k=3}^N c_k E[He_{k-1}(U) He_{n-1}(U)]$$

$$+ \frac{n(n-1)}{2} \sum_{k=3}^N c_k c_m E[He_{k-1}(U) He_{m-2}(U)]$$

in which the approximations are exact to second order in c_n ($n \geq 3$). The latter equality uses the relation $X_0/\kappa - U = \sum_{n=3}^N c_n He_{n-1}(U)$ from Eq. A14, and the differential properties of He_n :

$$He_n'(u) \equiv \frac{d^k He_n(u)}{du^k} = \frac{n!}{(n-k)!} He_{n-k}(u) \quad (\text{A17})$$

$$\varphi^{(k)}(u) \equiv \frac{d^k \varphi(u)}{du^k} = (-1)^k He_k(u) \varphi(u) \quad (\text{A18})$$

(Eq. A18, in which φ is the standard normal density, is found useful below.)

The corresponding orthogonal polynomial moments, now defined as "Hermite" moments h_n , are given by $h_n = E[He_n(X_0)]/n!$ from Eq. A4. The numerator of this result can be evaluated from Eq. A16, whose first two terms are simply zero and $n c_n E[He_{n-1}^2(U)] = c_n n!$ in view of orthogonality. The result can be written as

$$h_{p+2} = c_{p+2} + \frac{1}{2p!} \sum_{k=3}^N c_k c_m E[He_{k-1}(U) He_{m-1}(U) He_p(U)] \quad (\text{A19})$$

for $1 \leq p \leq N-2$. Integrating by parts, the Hermite triple product may be reduced to a series of double products:

$$E[He_{k-1}(U)He_{m-1}(U)He_p(U)] = \int_{-\infty}^{+\infty} He_{k-1}(u)He_{m-1}(u)He_p(u)[He_p(u)\varphi(u)]du$$

$$\begin{aligned} \text{Eq. A18:} &= \int_{-\infty}^{+\infty} He_{k-1}(u)He_{m-1}(u)(-1)^p \varphi^{(p)}(u) du \\ &= \int_{-\infty}^{+\infty} [He_{k-1}(u)He_{m-1}(u)](\varphi)^{(p)}(u) du \end{aligned} \tag{A20}$$

$$p \text{ uses of product rule: } = \sum_{j=0}^p \frac{p!}{j!(p-j)!} \int_{-\infty}^{+\infty} He_k^{(j)}(u)He_m^{(p-j)}(u)\varphi(u)du$$

The mean derivatives may then be evaluated from Eq. A17:

$$\begin{aligned} E[He_{k-1}^{(j)}(U)He_m^{(p-j)}(U)] &= \frac{(k-1)!}{(k-1-j)!} \frac{(m-1)!}{(m-1-p+j)!} E[He_{k-1-j}(U)He_{m-1-p+j}(U)] \\ &= \frac{(k-1)!(k-1+p-2j)!}{(k-1-j)!} \end{aligned} \tag{A21}$$

for $m=k+p-2j$, and zero for other values of m .

The final result is obtained by substituting this result into Eq. A20 and then into Eq. A19. In view of Eq. A21, the summation over m in Eq. A19 has nonzero contribution only from a single term ($m=k+p-2j$). Switching the remaining summations over p and k , we find that

$$h_{p+2} = c_{p+2} + \frac{1}{2} \sum_{j=0}^p \frac{1}{j!(p-j)!} \sum_k c_k c_{k+p-2j} \frac{(k-1)!(k-1+p-2j)!}{(k-1-j)!} \tag{A22}$$

The summation over the index k should include all available coefficients c_3, \dots, c_N . This leads to two ranges of k values: $3 \leq k \leq N - |p-2j|$ for $p \geq 2j$, and $3 + |p-2j| \leq k \leq N$ for $p \leq 2j$. So that we may adopt the former range for all j values, in the latter case we replace k by $k-p+2j$ in the summand of Eq. A22:

$$\begin{aligned} p \geq 2j: & c_k c_{k+p-2j} \frac{(k-1)!(k-1+p-2j)!}{(k-1-j)!} \\ p \leq 2j: & c_{k-p+2j} c_k \frac{(k-1-(p-2j))!(k-1)!}{(k-1-p+j)!} = c_k c_{k+p-2j} \frac{(k-1)!(k-1+|p-2j|)!}{[k-1-(p-|p-2j|)]/2!} \end{aligned}$$

With this substitution we arrive at Eq. 14a, with c_k written as \tilde{h}_k to emphasize its similarity to the Hermite moment h_k . For $p=1$ and 2, for example, we find

$$\begin{aligned} p=1: & h_3 - c_3 = \sum_{k=3}^{N-1} k! c_k c_{k+1} = 6c_3 c_4 + \dots \\ p=2: & h_4 - c_4 = \frac{1}{2} \left[\sum_{k=3}^N (k-1)! c_k^2 + \sum_{k=3}^{N-2} (k+1)! c_k c_{k+2} \right] = 2c_3^2 + 9c_4^2 + \dots \end{aligned} \tag{A23}$$

If $N=4$ moments are to be fit, the terms shown explicitly give the complete relations between the unknown parameters c_3 and c_4 and the higher moments

$h_3 = \alpha_3/6$ and $h_4 = (\alpha_4 - 3)/24$. With the approximate back-substitution approach described following Eq. 14, the term $2c_3^2$ is ignored and Eq. 15 is obtained for c_3 and c_4 (i.e., \tilde{h}_3 and \tilde{h}_4).

ORTHOGONAL POLYNOMIALS		
Parent process, $U(t)$:	Normal	Chi-Square -2
$f \varphi(x)$:	$(2\pi)^{-1/2} \exp(-u^2/2)$	$\exp(-u) \quad (u \geq 0)$
$P_0(x)$:	1	1
$P_1(x)$:	x	$x-1$
$P_2(x)$:	x^2-1	x^2-4x+2
$P_3(x)$:	x^3-3x	$x^3-9x^2+18x-6$
$P_4(x)$:	x^4-6x^2+3	$x^4-16x^3+72x^2-96x+24$
$P_5(x)$:	x^5-10x^3+15x	$x^5-25x^4+200x^3-800x^2+600x-120$
General Results		
$P_n(x)$:	$x^n - \frac{n!x^{n-2}}{1!2!(n-2)!} + \frac{n!x^{n-4}}{2!2^2!(n-4)!} - \dots$	$x^n - 1![(n-1)!]^2 + 2![(n-2)!]^2 \dots$
$E[P_n^2(U)]$:	$n!$	$(n!)^2$
$P_n(0)$:	$P_{2n}(0) = (-\frac{1}{2})^n \frac{2n!}{n!}; P_{2n+1}(0) = 0$	$P_n(0) = (-1)^n n!$
Alternate Definitions		
$P_n(x)$:	$(-1)^n e^{x^2} \frac{d^n}{dx^n} (e^{-x^2})$	$(-1)^n e^x \frac{d^n}{dx^n} (x^n e^{-x})$
Recurrence Relations		
	$P_{n+1}(x) = xP_n(x) - nP_{n-1}(x)$	$P_{n+1}(x) = (x-2n-1)P_n(x) - n^2 P_{n-1}(x)$
	$P_n'(x) = nP_{n-1}(x)$	$xP_n'(x) = nP_n(x) + n^2 P_{n-1}(x)$

Table A-1: Orthogonal polynomials for normal and chi-square-2 processes.

Appendix B:

INCLUDING DEPENDENCE AND NONSTATIONARITY
IN MOMENT-BASED ESTIMATES
OF UPCROSSING RATES

It is useful in various applications to estimate $\nu_X(\tau)$, the mean rate at which the dynamic response $X(t)$ crosses the "resistance" level τ from below. Because the primary goal in the text has been to utilize only marginal (static) moments of $X(t)$, both Charlier and Hermite estimates of $\nu_X(\tau)$ have been based on specific dynamic models (Eqs. 1a and b, respectively). These assumptions regarding dynamic behavior can be relaxed if joint moments of $X(t)$ and $\dot{X}(t)$ are known. Nonstationarity of $X(t)$ can also be modelled through the time variation of these moments. Such general moment-based estimates of $\nu_X(\tau)$ are constructed in this appendix.

The basis for calculating $\nu_X(\tau)$ from the joint distribution of $X(t)$ and $\dot{X}(t)$ has been established by Rice (1944). The underlying principle is that if $X(t)$ is a smooth (differentiable) response, the likelihood of multiple up-crossings of level τ in an interval becomes negligible as its duration, dt , approaches zero. Therefore, as $dt \rightarrow 0$ the mean number of such up-crossings, $\nu_X(\tau)dt$, approaches the probability of one such crossing:

$$\nu_X(\tau)dt \rightarrow P[X(t) < \tau(t) \text{ and } X(t+dt) \geq \tau(t+dt)] \quad (dt \rightarrow 0) \quad (B1)$$

This includes the possibility that the resistance level, τ , may vary with time. (Formally, Eq. B1 should be viewed as an asymptotic relation, and $\nu_X(\tau)$ defined as the limiting ratio between the probability of an up-crossing and dt .)

We now enumerate all combinations of $X(t)$ and $\dot{X}(t)$ that lead to a crossing as defined in Eq. B1. Denoting $X(t)$ and $\tau(t)$ simply by X and τ and their time-derivatives at t by \dot{X} and $\dot{\tau}$, Eq. B1 can be simplified by replacing $X(t+dt)$ and $\tau(t+dt)$ in the limit by $X+\dot{X}dt$ and $\tau+\dot{\tau}dt$:

$$\begin{aligned} \nu_X(\tau)dt &= P[X < \tau \text{ and } X+\dot{X}dt \geq \tau+\dot{\tau}dt] \\ &= P[\dot{X} > \dot{\tau} \text{ and } \tau - (X-\tau)dt \leq X < \tau] \end{aligned}$$

$$= \int_{\dot{X}=\dot{\tau}}^{\infty} \int_{X=\tau-(\dot{X}-\dot{\tau})dt}^{\tau} f_{X,\dot{X}}(x,\dot{x}) dx d\dot{x} \quad (dt \rightarrow 0) \quad (B2)$$

This permits evaluation of $\nu_X(\tau)$ from the joint density, $f_{X,\dot{X}}(x,\dot{x})$. In the limit the inner integral becomes simply $(\dot{x}-\dot{\tau})f_{X,\dot{X}}(\tau,\dot{x})d\dot{x}$; substituting into

Eq. B1 and cancelling a common factor of dt gives

$$\nu_X(\tau) = \int_{\dot{x}=-\tau}^{\dot{x}=\tau} (\dot{x} - \tau) f_{X,\dot{X}}(\tau, \dot{x}) d\dot{x} \tag{B3}$$

This is conventionally known as "Rice's formula." The ratio $\nu_X(\tau)/f_X(\tau)$ may then be expressed in terms of either the conditional cumulative distribution $G_{\dot{X}|X}(\dot{x}|\tau) = P[\dot{X} > \dot{x} | X = \tau]$ or its derivative, the conditional probability density $f_{\dot{X}|X}(\dot{x}|\tau) = -\partial G_{\dot{X}|X}(\dot{x}|\tau)/\partial \dot{x}$:

$$\frac{\nu_X(\tau)}{f_X(\tau)} = \int_{\dot{x}=-\tau}^{\dot{x}=\tau} (\dot{x} - \tau) f_{\dot{X}|X}(\dot{x}|\tau) d\dot{x} = \int_{\dot{x}=\tau}^{\dot{x}=-\tau} G_{\dot{X}|X}(\dot{x}|\tau) d\dot{x} \tag{B4}$$

Integration by parts provides the latter result. If $X(t)$ and $\dot{X}(t)$ are independent random variables, Eq. B4 does not depend on τ so that $\nu_X(\tau)$ and $f_X(\tau)$ become proportional, as in Eq. 1a.

To estimate $\nu_X(\tau)$ from joint moments of $X(t)$ and $\dot{X}(t)$, a two-dimensional Charlier series for $f_{X,\dot{X}}(x, \dot{x})$ analogous to Eq. 2 can be used:

$$f_{X,\dot{X}}(x, \dot{x}) = \varphi(x) \varphi(\dot{x}) \sum_{n=0}^{\infty} \sum_{m=0}^{\infty} h_{nm} H_{e_n}(x) H_{e_m}(\dot{x}) \tag{B5}$$

in which H_{e_n} and H_{e_m} are Hermite polynomials, φ is the standard normal density, and h_{nm} is the joint Hermite moment.

$h_{nm} = \frac{E[H_{e_n}(X)E[H_{e_m}(\dot{X})]]}{n!m!}$ \tag{B6}

The orthogonality property, $E[H_{e_n}(U)H_{e_m}(U)] = n! \delta_{nm}$, can be used to show that the joint density in Eq. B5 has the following properties:

- Its moments are consistent with Eq. B6. This may be demonstrated as in Eq. A6, which shows that the univariate density in Eq. A5 yields the moments in Eq. A4.
- It produces the marginal distribution $f_X(x) = \varphi(x) \sum_{n=0}^{\infty} h_{n0} H_{e_n}(x)$, in terms of the scalar Hermite moments, h_{n0} , of $X(t)$. This is analogous to the univariate Charlier series for $f_{X_0}(x)$ in Eq. 2.
- Eq. B5 encloses volume $h_{00} = 1$, although it need not remain positive for all x and \dot{x} .

Note that if X and \dot{X} are independent, h_{nm} factors into $h_n \delta_{nm}$, the product of scalar Hermite moments of $X(t)$ and $\dot{X}(t)$. Also, because $H_{e_n}(x) = n! H_{e_{n-1}}(x)$, h_{n1} is proportional to the mean velocity of $H_{e_{n+1}}(X)$:

$$h_{n,1} = \frac{1}{n!} E[H_{e_n}(X)\dot{X}] = \frac{1}{(n+1)!} E\left[\frac{d}{dt} \{H_{e_{n+1}}(X)\}\right] = -\frac{1}{(n+1)!} \frac{d}{dt} E[H_{e_{n+1}}(X)] \tag{B7}$$

In particular, $h_{n,1} = 0$ for all n if $X(t)$ is stationary.

To estimate $\nu_X(\tau)$ from the Hermite moments h_{nm} , we substitute Eq. B5 into Eq. B4:

$$\begin{aligned} \nu_X(\tau) &= \int_{\dot{x}=\tau}^{\dot{x}=-\tau} f_X(\tau) G_{\dot{X}|X}(\dot{x}|\tau) d\dot{x} = \int_{\dot{x}=\tau}^{\dot{x}=-\tau} \int_{y=\tau}^{\dot{x}} f_{X,\dot{X}}(\tau, y) dy d\dot{x} \\ &= \varphi(\tau) \sum_{n=0}^{\infty} H_{e_n}(\tau) \sum_{m=0}^{\infty} h_{nm} \int_{\dot{x}=\tau}^{\dot{x}=-\tau} \int_{y=\tau}^{\dot{x}} H_{e_m}(y) \varphi(y) dy d\dot{x} \end{aligned} \tag{B8}$$

Because $H_{e_n}(x)\varphi(x) = (-1)^n \varphi^{(n)}(x)$, it follows that $\int_{\dot{x}} H_{e_n}(y)\varphi(y) dy$ is equal to $H_{e_{n-1}}(x)\varphi(x)$ for $n > 0$. Eq. B8 then becomes

$$\nu_X(\tau) = \frac{1}{2\pi} \exp\left(-\frac{\tau^2}{2}\right) \sum_{n=0}^{\infty} c_n H_{e_n}(\tau) \tag{B9}$$

in which the coefficients c_n are given by

$$c_n = \exp\left(-\frac{\tau^2}{2}\right) \left[h_{n0} [1 - \tau R(\tau)] + h_{n,1} R(\tau) + \sum_{m=0}^{\infty} h_{n,m+2} H_{e_m}(\tau) \right] \tag{B10}$$

in which $R(x) = \Phi(-x)/\varphi(x)$ is Mill's ratio, the reciprocal of the hazard function for the half-normal distribution. $R(x)$ can be calculated by evaluating Φ and φ , or through various direct approximations (e.g., Chapter 33 of *Johnson and Kotz, 1970*).

Eqs. B9-B10 provide a general result for $\nu_X(\tau)$, in which the weighting coefficients c_n reflect changes in resistance level through τ and nonstationarity through time-varying h_{nm} . Various simplifications may arise in practice. If the resistance level remains constant, for example, $\dot{\tau} = 0$ and $H_{e_{2n}}(\tau)$ becomes $H_{e_n}(0) = (-1/2)^n (2n)!/n!$ (e.g., Table A-1). In this case only even values of m contribute to the summation in Eq. B10, which can be rewritten with m replaced by $2m$:

$$c_n = h_{n,0} + \sum_{m=0}^{\infty} \frac{2m!}{m!} \left(-\frac{1}{2}\right)^m h_{n,2m+2} + \sqrt{\frac{\pi}{2}} h_{n,1} \tag{B11}$$

If $X(t)$ is also stationary, $h_{n,1} = 0$ (Eq. B7) and Eqs. B9-11 simplify further, leading to the result cited in Eq. 6 of the main text.

Standardized Responses. In practical applications, it is important that expansions such as Eq. B5 converge relatively quickly, so that reasonable accuracy can be achieved with a limited number of terms. This rate of convergence is generally increased by first standardizing the response and its velocity, so that its first two moments agree with those of the "parent" probability density, φ . Standardization may also aid in interpreting these results.

In general, both the mean and standard deviation of $X(t)$, $\mu_X(t)$ and $\sigma_X(t)$, will vary with time. Nonetheless, the standardized response $X_0(t) = [X(t) - \mu(t)]/\sigma(t)$ will have zero mean and unit variance for all t . Moreover, after standardization the response velocity $\dot{X}_0(t)$ has zero mean and is uncorrelated with $X_0(t)$:

$$E[\dot{X}_0] = E\left[\frac{dX_0}{dt}\right] = \frac{d}{dt} E[X_0] = 0 \quad (B12)$$

$$E[X_0\dot{X}_0] = E\left[\frac{d}{dt}\left(\frac{X_0^2}{2}\right)\right] = \frac{d}{dt} \left[\frac{E[X_0^2]}{2}\right] = 0$$

The final equalities follow because $E[X_0] = 0$ and $E[X_0^2] = 1$ for all t . To standardize the velocity as well, we need to calculate $\text{Var}[\dot{X}_0]$. Differentiating $X = \mu_X + \sigma_X X_0$, we find $\dot{X} = \dot{\mu}_X + \sigma_X \dot{X}_0 + \dot{\sigma}_X X_0$; because these terms are uncorrelated, their variances can be added and solved for $\text{Var}[\dot{X}_0]$:

$$\text{Var}[\dot{X}_0] = \frac{\sigma_X^2 - \dot{\sigma}_X^2}{\sigma_X^2} = \omega_0^2 \quad (B13)$$

This gives a useful definition of a representative circular frequency ω_0 , consistent with the ideally narrow-band case in which $X_0 = \sqrt{2} \cos(\omega_0 t + \psi)$.

In analogy to Eqs. B5 and B6, the joint probability density of $X_0(t)$ and $V_0(t) = \dot{X}_0(t)/\omega_0$ can be expanded as

$$f_{X_0, V_0}(x_0, v_0) = \varphi(x_0)\varphi(v_0) \left[1 + \sum_{n=2}^{\infty} \sum_{m=n-2}^{\infty} h_{nm}^0 He_n(x_0) He_m(v_0) \right] \quad (B14)$$

in which

$$h_{nm}^0 = \frac{E[He_n(X_0)E[He_m(V_0)]]}{n!m!} \quad (B15)$$

The superscript zero in Eq. B15 indicates that, unlike Eq. B6, the variables are standardized before the Hermite moment is calculated (as with the scalar Hermite moments h_n of $X(t)$ in the main text). Eq. B14 uses the fact that if $m+n=1$ or 2, $h_{nm}^0 = 0$ for all t due to standardization, even if $X(t)$ is nonstationary. Substituting this result into an expression analogous to Eq. B8 for $\nu_X(\tau)$:

$$\nu_X(\tau) = \omega_0 \int_{v=-\tau_0^0/\omega_0}^{\tau_0^0/\omega_0} \int_{v_0=0}^{\tau_0^0/\omega_0} f_{X_0, V_0}(v_0, v_0) dv_0 dv_0 \quad (B16)$$

$$= \frac{\omega_0}{2\pi} \exp\left(-\frac{\tau_0^2}{2}\right) \sum_{n=0}^{\infty} c_n He_n(\tau_0)$$

in which

$$c_n = \exp\left(-\frac{\Delta^2}{2}\right) \left[h_{n0}^0 [1 - \Delta R(\Delta)] + h_{n1}^0 R(\Delta) + \sum_{m=0}^{\infty} h_{n, m+2}^0 He_m(\Delta) \right] \quad (B17)$$

and in which $\tau_0^0 = (\tau - \mu_X)/\sigma_X$ is the standardized threshold and $\Delta = \tau_0^0/\omega_0$ is roughly the change in this threshold per cycle. Note that if the response is nonstationary τ_0 will generally vary with time even if the original resistance level, τ , does not. If nonstationary aspects evolve slowly, however, Δ may be small and a linearized form of Eq. B17 may suffice:

$$c_n = h_{n0}^0 + \sum_{m=0}^{\infty} \frac{2m!}{m!} \left(-\frac{1}{2}\right)^m h_{n, 2m+2}^0 \quad (B18)$$

$$+ \sqrt{\frac{\pi}{2}} h_{n1}^0 + \left[\sum_{m=0}^{\infty} \frac{(2m+1)!}{m!} \left(-\frac{1}{2}\right)^m h_{n, 2m+3}^0 - \sqrt{\frac{\pi}{2}} h_{n0}^0 - h_{n1}^0 \right] \Delta + O(\Delta^2)$$

If $X(t)$ is stationary and the resistance τ is constant, $\Delta = h_{n1}^0 = 0$ so that the second line of Eq. B18 is zero. The first line, therefore, gives weighting coefficients for stationary responses' upcrossing rates; the first term accounts for marginal response moments (i.e., h_{n0}^0), and the latter summation reflects joint statistics of response and its velocity through $h_{n, 2m+2}^0$. The second line of Eq. B18 includes corrections for slowly evolving nonstationarity. Finally, in the special case of linear/normal responses, $h_{nm}^0 = 0$ if $m+n > 0$ so that

$$\nu_X(\tau) = \frac{\omega_0}{2\pi} \exp\left(-\frac{\tau_0^2 + \Delta^2}{2}\right) [1 - \Delta R(\Delta)] \quad (B19)$$

$$= \frac{\omega_0}{2\pi} \exp\left(-\frac{\tau_0^2}{2}\right) \left(1 - \sqrt{\frac{\pi}{2}} \Delta + \frac{1}{2} \Delta^2 + \dots\right)$$

In the nonstationary case ω_0 , τ_0 , and Δ may all vary with time; in the stationary case $\Delta = 0$ and these other quantities remain constant.

Generalized Moment-Based Hermite Series. Even if the response is standardized, Charlier estimates of $\nu_X(\tau)$ from a limited number of marginal response moments cannot reflect significant nonnormality (e.g., Figs. 1-3). We may expect similar limitations to the more general Charlier models constructed here from joint moments of $X(t)$ and $\dot{X}(t)$, because they too estimate the ratio between true and normal upcrossing rates (Eqs. B16-B17 and B19) by a low-order poly-

mial in τ_0 .

Alternative results have been found from marginal response moments through Hermite models, which fit a Hermite series transformation of a normal (linear) response (e.g., Eqs. 7 and 16). Corresponding estimates of static statistics (e.g., $f_X(x)$) and dynamic statistics (e.g., $\nu_X(x)$) are considerably more flexible than those of the Charlier series (Figs. 1-3). In the dynamic case, however, these Hermite series use a specific dynamic model (Eq. 1b) which, if incorrect, may produce less accurate estimates of $\nu_X(x)$ than of $f_X(x)$. (These errors are often conservative, as in Fig. 5.)

Joint moments of the response and its velocity, if available, provide knowledge of actual dynamic behavior. It is therefore useful to combine the Hermite models, which accurately reflect static behavior, with the foregoing dynamic corrections for $\nu_X(x)$ that include these joint moments. Specifically, using the static Hermite model for the standardized PDF $f_{X_0}(x_0)$ (Eq. 11) and the Charlier estimate of the dynamic correction $\nu_{X_0}(x_0)/f_{X_0}(x_0)$ (ratio of Eq. B16 to Eq. 2), the product gives the upcrossing rate

$$\nu_X(x) = \nu_{X_0}(x_0) = \frac{\dot{u}_0^2(x_0)}{2\pi} \exp\left(-\frac{u^2(x_0)}{2}\right) \frac{d\dot{u}}{dx_0} \frac{\sum_{n=0}^{\infty} c_n H e_n(x_0)}{\sum_{n=0}^{\infty} h_n H e_n(x_0)} \quad (\text{B20})$$

in which $x_0 = (x - \mu_X)/\sigma_X$ is the standardized threshold, h_n is the marginal Hermite moment in Eqs. 3 and 4a, and $u(x_0)$ and $d\dot{u}/dx_0$ are given explicitly by Eqs. 16 and 17a, and implicitly by Eqs. 7 and 8a, for hardening and softening Hermite models, respectively. Through the coefficients c_n in Eqs. B17 and B18, the static Hermite model is generalized to reflect joint moments of $X(t)$ and $\dot{X}(t)$, nonstationarity, and time-varying thresholds.

To illustrate the potential increase in accuracy, consider the response of an oscillator with nonlinear stiffness to white noise excitation (Fig. 5). In this case $X(t)$ and $\dot{X}(t)$ are independent, so that c_n is proportional to h_n and the ratio of summations in Eq. B20 becomes independent of x_0 . Eq. B20 then correctly predicts that ν_X and f_X are proportional. Consequently, Eq. B20 reduces the Hermite estimate of $\nu_{X_0}(x_0)/f_{X_0}(0)$, from the overly conservative result shown in Fig. 5, to agree with the corresponding Hermite estimate of $f_{X_0}(x_0)/f_{X_0}(0)$. This leads to closer agreement with the trend shown by actual upcrossing rates for various forms of the nonlinear stiffness.